INTERNATIONAL ATOMIC ENERGY AGENCY
UNITED NATIONS EDUCATIONAL, SCIENTIFIC AND CULTURAL ORGANIZATION
INTERNATIONAL CENTRE FOR THEORETICAL PHYSICS
I.C.T.P., P.O. BOX 586, 34100 TRIESTE, ITALY, CABLE: CENTRATOM TRIESTE

SMR/459 - 2

SPRING COLLEGE IN CONDENSED MATTER ON: PHYSICS OF LOW-DIMENSIONAL SEMICONDUCTOR STRUCTURES

(23 APRIL - 15 JUNE 1990)

QUANTUM WELLS AND SUPERLATTICES: AN OVERVIEW

G. Bastard
Département de Physique
ENS
24 Rue L'homond
F-75005 Paris
France

QUANTUM WELLS AND SUPERLATTICES: AN OVERVIEW

G. Bastard

Département de Physique ENS. 24 rue Lhomond. F-75005 Paris (France).

Abstract

We shall present a broad coverage of the electronic properties of semiconductor superlattices emphasizing electric field effects (Quantum Confined Stark Effect and Wannier-Stark quantisation). The following notes are part of an article[1] to be published in Solid State Physics.

1) G. Bastard, J. A. Brum and R. Ferreira. To be published in Solid State Physics

V. Stark Effects in Semiconductor Quantum Wells and Superlattices

V.1. Introduction

The previous paragraphs have been devoted to a presentation of the electronic structure of heterolayers under flat band condition. In this section we consider the case where an external and constant electric field is superimposed to the band edge profile of the heterostructure. We confine our discussion to a theoretical description of Stark shifts in semiconductor quantum wells and superlattices. In the first kind of structures the field leads to a red shift of the ground electron and hole states and thus of the fundamental band-to-band transition[116,117]. In superlattices instead, the electric field leads to a blue shift[125,126] of the band to band absorption edge. The opposite signs of the two effects stem in their different physical origin. In quantum wells there is a field-induced polarization[116] of the bound eigenstates and thus a nearly quadratic energy shift due to the interaction of the induced dipole with the field. In superlattices, the field suppresses the tunnelling between the consecutive wells[125] and thus isolates the different wells from each others. Thus, the lowest lying optical transition occurs in strong field between the levels of quasi-independent wells while at zero field it takes place between the lowest lying eigenstates of interacting wells which, as shown in the previous paragraphs, occur at an energy lower than roughly half of the electron or hole subband widths.

The Stark effect in isolated wells or superlattices have stimulated a significant amount of academic researches. They are also at the heart of novel opto-electronic devices (e.g. fast electro-optical modulators)[119-121]. In the following we shall first describe the Stark effect in isolated quantum wells, then in double quantum wells, which are the shorter possible superlattices and finally in superlattices

V.2. Electric field effects in isolated quantum wells

As pointed out in the introduction there is a rich technological potential in application and switch of a longitudinal (F//z) electric field to quantum wells. The usefulness of these structures lays in their capability of standing large electric fields ($F \leq 10^5$ V/cm), which produce large Stark shifts, while still displaying quasi discrete bound states.

We shall assume that the field is uniform over the whole structure, as approximately realized when the quantum well is inserted in the

intrinsic part of a reverse-biased p-i-n junction or in the depletion length of a reverse-biased Schottky diode. In the case of multiple quantum wells, the barrier separating two consecutive wells will be assumed thick enough to prevent any sizeable coupling between their eigenstates. Thus, neglecting band mixing effects, the Schrödinger equation we have to investigate is

$$[-h^2/2m^* d^2/dz^2 + V_b(z) + eFz\ ]\chi(z) = \varepsilon\,\chi(z) \qquad (V\text{-}1)$$

In eq. (V-1) the in-plane motion has been dropped, $V_b(z)$ is the potential energy profile of a single rectangular quantum well and the electrostatic potential eFz has been set equal to zero at the center of the quantum well. It may sometimes be more convenient to take its origin on the left hand side (l.h.s.) corner of the well. A constant electric field leads to pathological behaviour of the eigenstates of eq.(V-1) versus F. At zero field the Schrödinger equation admits at least one bound state ($\varepsilon < V_b$) while an arbitrarily small F is sufficient to transform the allowed energy spectrum into a continuum. This is because the potential energy is arbitrary large and negative at large and negative z. Despite the lack of true bound states we expect, if F is not too large, that there will exist in the continuous spectrum some particular energies where the carrier wavefunction piles up in the quantum well[117,123]. Moreover, these particular energies will smoothly extrapolate to the true quantum well bound states when $F \rightarrow 0$. In fact, we do know from experiments that, over a significant field range (typically $F \leq 10^5$V/cm), the quantum well structures support states which behave as if they were truly bound. Thus, it is worth trying to convince ourselves that some stationary eigenstates of eq.(V-1) are indeed peculiar in that they display an accumulation of their wavefunctions in the well. An alternative description, which is often more revealing, is to consider them as metastable (i.e. non stationary) solutions of the time dependent tilted quantum well problem. This kind of description is relevant when the decay time of the quasi bound states is long. Hereafter, we shall also denote the peculiar stationary solutions of eq.(V-1) as the metastable state, since it can be shown that the real part of the complex eigenenergies of the time-dependent problem coincide with the (real) energies of the peculiar solutions of eq.(V-1).

Apart from the exact, Airy-like solutions, there are various ways to find the metastable states of eq.(V-1). Firstly, one may cut the electric field at some large distance from the investigated quantum well (fig. 45) and impose the existence of an infinite barrier. The problem

becomes that of finding true bound states in a complicated band edge profile. The outcome of such calculations is that there exists a large number of states which are essentially localized in the large triangular well and show a very small probability of being in the well. A small number of states are found to display an enhanced probability of being in the well. These are the metastable states whose energy positions extrapolate smoothly to those of the zero field bound states of the well.

One may also cut the electric field at some large distances on both sides of the well and investigate the transmission coefficient $T(\varepsilon) = |t(\varepsilon)|^2$ of a plane wave with unity amplitude impinging at $z = - \mathcal{L}$ on the barrier and being finally transmitted at $z = + \mathcal{L}$. $T(\varepsilon)$ is very low (because $\mathcal{L}$ is large) except in the vicinity of some energies which belong to the segment $[\eta_1, \eta_2]$ where it displays sharp peaks ($T \leq 1$). As usual, these transmission resonances[117] correspond to the trapping of the particle inside the the quantum well. If the resonances are narrow this means that the corresponding trapping times τ_{trap} are long : $\tau_{trap}\, \Delta E > h/2$ where ΔE is the width of the resonance.

Another way to depict these resonances is to consider them as virtual (or metastable) bound states[35,123], i.e. as bound states of the quantum well with a complex energy $E_n - ih/2\tau_{trap}$. The reason why the energies of these states have to be complex and not purely real is that the solutions of the Schrödinger equation eq.(V-1) with the boundary conditions corresponding to a piling up of the wavefunction at $t = 0$ in the quantum well and to an outgoing wave at $z = - \infty$ do not fulfill the requirement of the probability current conservation, i.e. are not stationnary. On the other hand, it can be shown[35] that such solutions are approximate eigenstates of eq.(V-1) provided their energies are complex.

In order to set up a criterion allowing us to neglect, in a first approximation, the escape of the particle outside the quantum well, the condition

$$eF\kappa_b^{-1} \ll V_b - E_1 \qquad (V\text{-}2)$$

was proposed some time ago[116], where E_1 is the confinement energy in the quantum well and κ_b^{-1} the characteristic decay length of the bound state wavefunction at zero field. The meaning of eq.(V-2) is that the lowering of the barrier by the field over the characteristic decay length of the zero field wavefunction must remain negligible with respect to the effective F=0 barrier height $V_b - E_1$.

One can derive a similar criterion by looking at the problem from a different angle. Suppose we know that we have built up at t = 0 a quasi bound state E_1, which, if the l.h.s. barrier were flat, would be truly bound. Correspondingly, the particle would (classically) oscillate back and forth in the well for ever with a period $T(E_1)$. Since, however, the l.h.s. barrier is tilted the electron which oscillates in the well progressively escapes to infinity. Using the same semi-classical approach as in section III, we get:

$$1/\tau_{esc.}=D(E_1)\ /T(E_1) \qquad (V\text{-}3)$$

where $D(E_1)$ is the transmission of the tilted barrier. In the semiclassical approximation $D(E_1)$ is given by:

$$D(E_1) = D_0 \exp\{ -(4/3eF)\ (2m^*/h^2)^{1/2}\ (V_b-E_1)^{3/2} \} \qquad (V\text{-}4)$$

with $D_0 \approx 1$. As for the evaluation of $T(E_1)$ one gets :

$$T(E_1) = 4/eF(m^*E_1/2)^{1/2} \qquad \text{if } E_1<eFL \qquad (V\text{-}5)$$

$$T(E_1) = 4/eF(\ m^*E_1/2\ )^{1/2}\ x[(1 + (1-eFL/E_1)^{1/2}] \qquad \text{if } E_1 \geq eFL \qquad (V\text{-}6)$$

The lifetime $\tau(E_1)$ will be long if the argument of the exponential in eq.(V-5) is large and negative, which means :

$$V_b- E_1 >> 3/4\ eF\kappa_b^{-1} \qquad (V\text{-}7)$$

which (apart from the factor 3/4) is just the criterion we derived previously on the smallness of the barrier lowering by the field over the distance κ_b^{-1} where the wavefunction is important in the barrier.
Assuming that the lower bound for >> is 10 and taking V_b-E_1 = 0.125 eV, $m^* = 0.07m_0$ we find that eq.(V-7) is satisfied if $F < 7.93 \times 10^4$ V/cm. If, in addition, L = 100 Å, $D_0 \cong 1$ and E_1 = 70 meV, we get $h/2\tau_{esc}(E_1) \cong 2.5\ 10^{-4}$ meV and $\tau_{esc}(E_1) \cong 1.3$ ns. For these typical sample parameters the level broadening is still small with respect to the confinement energy. The escape lifetime is relatively long but is not much longer than a recombination lifetime ($\cong$1 ns). The capture of the carrier by some

shallow impurity may eventually be more efficient than the field-induced tunnelling. Notice finally the strong dependence ($F \exp(-F_c/F)$) of τ_{esc}^{-1} with the field. It arises from the transparency coefficient eq.(V-4). If instead of applying 8×10^4 V/cm we only apply 50 kV/cm, $\tau(E_1)$ increases by several decades and the field-induced tunnelling becomes a completely negligible effect with respect to recombination or capture phenomena. Figure (46) shows the calculated τ_{esc} versus F for E_1, HH_1 and LH_1 in GaAs-Ga(Al)As quantum wells with thicknesses 30 Å, 60 Å and 90Å. τ_{esc} is found to vary considerably (from 1ps to 1s) in the investigated field range. Moreover, fig.(46) clearly shows that the field-induced escape of the carrier outside the quantum well is practically negligible when L≥100Å. Most of the quantum well structures which have been so far investigated (e.g. in electro-absorption) have shown excellent performances (i.e. pronounced exciton peaks) in field up to $\cong 10^5$ V/cm. The previous considerations have aimed to point out why it could be so in spite of the field-induced tunnelling. From now on we shall neglect this effect and investigate the second useful feature of the electric field effects on quantum well states, which is the existence of large Stark shifts.

The zero-field eigenstates of eq.(V-1) may be classified according to the parity operator. Since the eFz is odd in z it only couples the zero-field eigenstates of opposite parities. Since we forget about field-induced tunnelling we may have recourse to perturbation or variational approaches[116,117] to calculate the field dependence of the eigenenergies. The basic physics is that the quantum well bound states become polarized by the electric field which in turn lead to a shift of their eigenenergies by $1/2\ \mathbf{D}_n.\mathbf{F}$ where $\mathbf{D}_n$ is the average value of the dipole operator in the n^{th} state. In the low field limit $\mathbf{D}_n = \alpha_n \mathbf{F}$ where α_n is a c-number. This results in a quadratic (Stark) shift upon F. For larger fields α_n becomes F-dependent displaying some saturation : D≅eL/2. This is the carrier accumulation regime where the wavefunction piles up near the l.h.s. of the well for electron and the right hand site (r.h.s.) for holes (see fig.47). This carrier accumulation is the useful feature for electro-optical devices : by inhibiting the carrier escape towards $\pm \infty$ (which is unavoidable in bulk materials) the quantum well walls give access to large (≅ 30 meV) energy shifts while preserving the carrier localization and thus the beneficial action of enhanced excitonic binding[117,122]. This effect has led to a number of electro-optical devices, e.g. fast modulators[119,120].

In the small field limit we can use a second order perturbation

approach to obtain:

$$E_n(F) = E_n(0) + e^2F^2 \sum_{m \neq n} |\langle m|z|n\rangle|^2/(E_n - E_m) \qquad (V\text{-}8)$$

where $|\ n\ \rangle$ is the n^{th} zero field bound eigenstate with energy $E_n(0)$ and where the summation over m runs over the zero field bound and unbound states. The latters give a small contribution and are usually neglected. From eq.(V-8) we see that the ground state (n=1) experiences a red shift, as always. Since $E_n - E_m \cong L^{-2}$ and $\langle n \mid z \mid 1 \rangle \cong L$, $E_1(F) - E_1(0)$ scales like $L^4F^2m^*$. But the domain of validity of eq.(V-8), which is that the field-induced shift remains small with respect to the unperturbed energy splittings, narrows like m^*FL^3 = constant. Once the field is too large to use eq.(V-8), one may use variational approaches. A linear variational treatment consists of expanding $\chi(z)$ on the uncomplete basis spanned by the zero-field bound eigenstates of eq.(V-1). In this way, one obtains the field dependences of all the states. In fig.(48) we show the outcome of such a calculation. If one is interested in the ground state only (as often in device applications), a non linear variational wavefunction like :

$$\chi(z) = \chi^{(0)}(z)\ \exp(-\beta z) \qquad (V\text{-}9)$$

is quite accurate, as it describes the tendency towards accumulation ($\beta > 0$ for electron; $\beta < 0$ for holes), and of simple use. In eq.(V-9) $\chi^{(0)}(z)$ is the ground bound solution of eq.(V-1) at zero field. The wavefunction given in eq.(V-9) also contains the signature of significant field-induced tunnelling : as $|\beta|$ increases with F it happens that it becomes larger than $\kappa_b(0)$ the zero-field wavevector characterizing the evanescent wing of the ground bound state. The minimization procedure becomes impossible and one may rightfully consider that the very notion of quasi discrete bound state fades away. To examplify the tunability range of energy level shifts upon the electric field we show in figs.(49,50) the calculated field dependence of the E_1-HH_1 interband energy for various well thicknesses L in GaAs-Ga(Al)As and Ga(In)As based quantum wells. It is seen that considerable shifts can be produced for L ≥100Å. The data obtained in GaAs quantum wells[127] are very well described by the calculations.

The electric field-induced polarization of the carrier wavefunctions suppresses their parity properties. Thus, optical transitions which were parity-forbidden at zero field become allowed at non vanishing F. Their growth occurs at the expense of the F=0 parity-allowed transitions. Miller et al[118] have very nicely discussed the

sum rules associated with optical transitions in biased quantum wells as well as the progressive evolution of the optical absorption lineshape from that of biased quantum wells to the Franz-Keldysh effect in thick, bulk-like, structures (L≥500Å).

V.3. Electric field effects in double quantum wells

The eigenstates of double quantum wells can accurately be obtained by diagonalizing the eFz term between all the zero field bound states of the problem (these states are analytically known). The physics is however more transparent if one attempts a tight binding expansion of the eigenstates on a basis spanned by all the zero field bound states of each well when considered as isolated[128]. For symmetrical double quantum wells one, for instance, would write:

$$\chi(z) = \sum_{i = \pm 1} \sum_{n} c_{i,n}\, \phi_{loc}^{(n)}(z - id/2) \qquad (V\text{-}10)$$

where d = L+h would be the period of the associated superlattice, L (h) being the quantum well (intermediate barrier) thickness and $\phi_{loc}^{(n)}(z-z_0)$ is the n^{th} bound state wavefunction of the quantum well centered at z_0 when considered as isolated and under flat band condition. To keep the matter simple, let us assume that the $\phi_{loc}^{(n)}$ are orthonormalized:

$$\langle \phi_{loc}^{(n)}(z - id/2) \mid \phi_{loc}^{(m)}(z - i'd/2) \rangle = \delta_{i,i'}\delta_{nm} \quad ; \quad i, i' = \pm 1 \qquad (V\text{-}11)$$

Then, in the case where the unbiased, isolated, wells admit two bound states (E_1 and E_2) the hamiltonian takes the matricial form:

$$\begin{pmatrix} E_1 - eFd/2 & \lambda_1 & eFZ_{12} & eFz_{12} \\ \lambda_1 & E_1 + eFd/2 & eFz_{12} & eFZ_{12} \\ eFZ_{12} & eFz_{12} & E_2 - eFd/2 & \lambda_2 \\ eFz_{12} & eFZ_{12} & \lambda_2 & E_2 + eFd/2 \end{pmatrix} \qquad (V\text{-}12)$$

where some terms have been dropped since they do not bring essential physical features and Z_{12} (respectively z_{12}) are the matrix elements of the z operator between $\phi_{loc}^{(1)}$ and $\phi_{loc}^{(2)}$ which are centered in the same well (respectively in different wells). The two diagonal 2x2 blocks express the couplings between the same sort of states (E_1 or E_2) in either

wells while the eFZ_{12} term is just the intra-well field dependent polarization (the one which gives rise to the Stark effect in isolated wells) and the eFz_{12} term is the inter-well field dependent polarization . z_{12} is in general smaller or much smaller than Z_{12} since the wavefunctions involved in the former matrix element peaks in different wells while those in the latter matrix element are both centered in the same well. λ_1 and λ_2 are the nearest neighbour transfer integrals between the wells corresponding to the ground and excited states respectively. If one neglects the off-diagonal blocks, which amounts to performing two one-band tight binding analysis separately, one gets immediately:

$$\varepsilon_{1,\pm} = E_1 \pm\sqrt{[(eFd/2)^2 + \lambda_1^2]} \qquad (V\text{-}13)$$

$$\varepsilon_{2,\pm} = E_2 \pm\sqrt{[(eFd/2)^2 + \lambda_2^2]} \qquad (V\text{-}14)$$

Equations.(V-13,14) are for the specific double well problem the equivalent of Wannier one-band tight binding analysis[129] of the superlattice eigenstates in an electric field. The physics behind eqs.(V-13,14) is the field induced turning off of the resonant tunnel coupling between wells and the concomitant localization of the eigenstates. What primarily does the field to the double well is to misaligne the levels of both wells by eFd while they were lined up at F = 0. If eFd exceeds the coupling terms between the wells (λ_1 for the ground state, λ_2 for the excited state), the tunnel effect between the wells becomes effectively non-resonant and thus weakens, to the extent that if F becomes very large there is no more coupling between the wells: the eigenenergies respectively converge towards $E_1 \pm 1/2eFd$ and $E_2 \pm 1/2eFd$ while their associated wavefunctions converges towards $\phi_{loc}^{(1)}(z \pm d/2)$ and $\phi_{loc}^{(2)}(z \pm d/2)$ respectively.

The second important physical feature exhibited by our simple model arises from the effect of the off-diagonal blocks on the eigenstates. When these blocks are absent there exists a crossing between ε_{1+} and ε_{2-} taking place at $F=F_c$ (where $eF_cd \equiv (E_2 - E_1)$ if $eF_cd/2 >> \lambda_1, \lambda_2$). This crossing is actually replaced by an anticrossing when the off-diagonal blocks are taken into account. If the field was strong enough to have localized both the E_1 and E_2 related states (i.e. if $1/2eF_cd >> \lambda_1, \lambda_2$) in either wells, the eigenstates again delocalize in a field range ΔF around F_c which strongly depends on the intermediate

barrier thickness: the thicker the barrier the smaller are the anticrossing and the departure of the eigenstates from a linear dependence upon F. In the field range $F_c \pm 1/2\Delta F$ a carrier assumed to be in the upper branch will make a very efficient relaxation towards the lower branch by emitting acoustical or optical phonons (energy conservation permitting) or by being elastically scattered in the lower branch and converting some of its longitudinal energy into transverse kinetic energy, this process being followed by a subsequent intra-lower branch desexcitation[128,131]. Of course, if the wells are not identical, the afore-mentionned anticrossings may as well take place between the ground, now unequivalent, bound states of both wells. Finally, the off diagonal blocks, mainly via the eFZ_{12} term, induce a deviation from a straight line dependence at large F ($F>>F_c$) of the eigenstates which is quadratic upon F. This is nothing but the intra-well Stark effect. Figure (51) displays the results of the field-dependent energies for a 100Å-20Å-100Å GaAs-$Ga_{0.7}Al_{0.3}As$ double quantum well (barrier height: 213 meV, $m^*= 0.07m_0$). The electrostatic potential is taken to vanish at the center of the middle barrier and the energy zero is taken at the bottom of the GaAs conduction band edge at F = 0. The states moving up (down) in energy are those which are mostly localized in the right hand side (left hand side) well. Figure (52) shows a plot of the spatial dependence of the 4 lower eigenstates of that structure for four different electric field strengths. At F = 0 the four levels are delocalized over the whole heterostructure. When F increases, the eigenstates become progressively localized in a given well, except near F_c where an anticrossing take place between ε_{1+} and ε_{2-}. When this anticrossing is passed through there is an interchange between the main spatial localizations of the second and third states respectively.

V.4. Electric field effects in superlattices

One of the original motivition for the growth of semiconductor superlattices was the hope of achieving a negative differential resistance by realizing a Bloch oscillator[1]. The Bloch oscillator, suggested in 1927[132], results from a semiclassical analysis of the electron motion in a potential which is the sum of a periodic term V(z) and a linearly varying term eFz. F is considered as so small that its effects can be treated semi-classically on the band structure defined by V(z). The fully quantum-mechanical version of the Bloch oscillator was derived by Wannier in the late 50's[129,133]. Wannier showed that a one band analysis of the problem leads to the replacement of the quasi continuous band spectrum of the crystalline solid (F=0) by a ladder of bound levels evenly

spaced by eFd where d is the period of the lattice along the electric field (Wannier-Stark ladder). Wannier's results were long disputed[134-141] on the ground that the electric field-induced interband mixing (Zener breakdown) would unavoidably wash out the ladders. Careful theoretical and numerical analysis[140] however showed that Wannier's findings were essentially correct, the interband couplings leading to a broadening of the bound levels into virtually bound ones. The width of the virtual bound states were estimated to be much smaller than the spacing eFd under many circumstances, thereby leading to the conclusion that the Wannier-Stark ladders could be in principle observable. In actual bulk samples, however, it was quickly realized that the time needed to complete a period of the semiclassical bound motion was considerably longer than any realistic collision time on impurities, defects, phonons etc..., thus leaving only a faint hope to observe this fascinating effect.

In fact, on the experimental side, the search for Wannier-Stark ladders proved to be elusive, although there has been reports on their observation in the early seventies in wide bandgap semiconductors[142]. Actually, the dominant effect of an electric field on the absorption edge of a bulk semeiconductor is the appearance of the Franz-Keldysh effect[143,144] (tail below the F=0 edge and oscillations above). These effects originate from the field-induced breakdown of the optical selection rules ($\Delta \mathbf{k}=\mathbf{0}$) along the electric field. Like in the Bloch oscillator model, the Franz-Keldysh formulae requires that the potential energy drop eFd over a lattice period remains much smaller than the bandwidths (or bandgaps), in order to treat the eFz term in a one band effective mass approximation.

Recently, Voisin[145] suggested to re-examine the Wannier-Stark problem in semiconductor superlattices from the point of view of the inhibition of the resonant tunnel effect between consecutive wells. He pointed out that this should result in an effective blue shift of the superlattice absorption edge. Bleuse et al[125] proved this idea to be algebraically correct and Mendez et al[126] and Voisin et al[146] experimentally demonstrated the existence of a blue shift in GaAs-Ga(Al)As superlattices. Since then, several experiments have evidenced various aspects of the Wannier-Stark quantization[147], including a room temperature achievement of an electro-optical switch utilizing the blue shift[148].

In the following we attempt a theoretical survey of the Wannier-Stark quantization in semiconductor superlattices. Efforts will be made to provide a comparison between the fully quantum treatment and the semiclassical one. We shall first discuss the simplest case which corresponds to the one band analysis made by Wannier and which is applicable to a good approximation to the conduction subbands of

superlattices whose wells, if they were isolated, would only support a single bound state (section V.4.a). Section (V.4.a) will also include short discussions of the intraband and interband optical properties associated with the Wannier-Stark states. The Wannier-Stark localization for the valence subbands of superlattices is again complicated by the $\mathbf{k}_\perp$-induced couplings between the light and heavy hole dispersions and by the fact that, usually, many subbands come into play due to the heavy hole mass. No analytical solutions appear thus manageable in the general case. The outcomes of numerical diagonalizations of the valence hamiltonian in biased but finite superlattices[149] are however sufficiently clear to allow the drawing of reliable conclusions about infinite superlattices. Section (V.4.b) will thus be devoted to the multiband effects on the Wannier-Stark quantization both for electrons and holes.

V.4.a. *The Wannier-Stark ladders*

We consider an infinite semiconductor superlattice subjected to a constant electric field. For simplicity we assume that the conduction states are built out of a single parabolic band which has the same symmetry (say Γ_6) for both host materials. The hamiltonian is written as:

$$H = T + \sum_n V(z-nd) + eFz \qquad (V\text{-}15)$$

where $V(z-nd)$ is the "atomic" square well potential felt in the superlattice period centered at $z = nd$. Consider the translation operators

$$\mathcal{T}_{jd} = \exp(ip_z jd/h) \qquad (V\text{-}16)$$

We find:

$$[\mathcal{T}_{jd}, H] = \mathcal{T}_{jd} H - H \mathcal{T}_{jd} = jeFd\, \mathcal{T}_{jd} \qquad (V\text{-}17)$$

Equation (V-17) states that the translation operators are no longer constants of motion if $F \neq 0$, a result physically arising from the potential energy drop $eFjd$ between two superlattice periods separated by jd. However, the fact that $[\mathcal{T}_{jd}, H]$ is proportional to $\mathcal{T}_{jd}$ itself implies that this operator evolves harmonically with the time. In particular, suppose that at time $t = 0$ the eigenstate of eq.(V-15) was also an eigenstate of $\mathcal{T}_{jd}$ with the eigenvalue $\exp(ik_0 jd)$. Then, eq.(V-17) shows that the

eigenstate of eq.(V-15) will remain an eigenstate of T_{jd} with the eigenvalue exp[ik(t)jd] where:

$$k(t) = k_0 - eFdt/h \qquad (V\text{-}18)$$

which is a rigourous justification of the "Newton" law of the semi-classical mechanics:

$$hdk/dt = -dV_{ext}/dz = -eF \qquad (V\text{-}19)$$

Notice that this law is exact only because the potential is linearly varying with z. Any other variation would not allow the generalization of eq.(V-19) to be exactly derivable.

When eq.(V-19) is used in conjunction with the definition of the velocity for a semi-classical electron:

$$\mathbf{v} = 1/h\partial\varepsilon_n/\partial\mathbf{k} \qquad (V\text{-}20)$$

the semi-classical equations of motion becomes entirely prescribed. In eq.(V-20) $\varepsilon_n(\mathbf{k})$ is the dispersion relation of the n^{th} subband (at zero field) and n is a constant of motion in the semi-classical analysis. Assuming a decoupling between the z and (x,y) motion, we obtain:

$$v_z(t) = \mathbf{v}.\mathbf{F}/F = 1/h\ \partial/\partial k_0[\varepsilon_n(k_0 - eFt/h)] \qquad (V\text{-}21)$$

which proves that both $v_z(t)$ and z(t) are periodic function of time with a period T_B equal to:

$$T_B = 2\pi h/eFd = 2\pi/\omega_B \qquad (V\text{-}22)$$

since $\varepsilon_n(q)$ is periodic upon q with periodicity $2\pi/d$. The oscillatory motion described by eqs.(V-21,22) is the Bloch oscillator and ω_B is the Bloch angular frequency. The Bloch oscillator is independent upon the exact shape of the dispersion relations $\varepsilon_n(q)$. To go one step further and obtain more explicit results, we restrict our attention to the ground subband $\varepsilon_1(q)$ derived from the ground bound state E_1 of the isolated wells. We adopt the simple but accurate tight binding expression for $\varepsilon_1(q)$:

$$\varepsilon_1(q) = E_1 - 2|\lambda|\cos(qd) \qquad (V\text{-}23)$$

The subband width Δ_1 is thus equal to $4|\lambda|$. From eqs.(V-21) we obtain:

$$v_z(t) = 2|\lambda|\, d/h \sin[(k_0 - eFt/h)d] \qquad (V\text{-}24)$$

$$z(t) = z_0 + 2|\lambda|/eF\cos[(k_0 - eFt/h)d] \qquad (V\text{-}25)$$

where z_0 is a constant of integration. The Bloch oscillator executes an harmonic motion with period T_B and amplitude $2|\lambda|/eF$ around its equilibrium position z_0. This oscillator is however peculiar in that its amplitude is unrelated to its total energy E_{tot} since E_{tot} is equal to $E_1 + eFz_0$ whereas for a regular harmonic oscillator (e.g. a mass m^* attached to a spring) one knows that the amplitude a is related to E_{tot} by $E_{tot} = 1/2 m^* a^2 \omega^2$, where ω is the angular frequency of the oscillator. The difference between both kinds of oscillator ultimately rests on the difference between the dependence of their kinetic energies upon the momentum. While the conventional oscillator can display an arbitrarily large kinetic energy, the Bloch oscillator one is bound by $E_1 + 2|\lambda|$. The latter property is closely associated with the counterintuitive response of the electron to an external field in the crystalline solid. While our intuition associates a constant acceleration to the electron motion in a constant field, the electron in the solid actually oscillates. The band structure (or the Bragg reflection effect) is still overwhelming in the semiclassical equations and falsifies our intuitive representation. Notice finally that the amplitude of the Bloch oscillator blows up when F vanishes. This raises the question of the applicablity of eqs.(V-24,25) to real superlattice structures, which are finite. The finite size effects could be incorporated in eq.(V-19) by adding, say, infinitely repulsive potential walls corresponding to both ends of the structure. We immediately see that, for such a finite structure comprising 2N + 1 periods, one should get $|z_0 \pm 2|\lambda|/eF| < (N + 1/2)d$ to ensure that eqs.(V-24,25) are still relevant. This criterion is better fulfilled for oscillators centered as far as possible from the edges ($z_0 = 0$) or for strong fields. Otherwise, one should numerically solve eqs.(V-19,20) to get the "edge-interacting Bloch oscillator" motions. Actually their period T_{edge} is equal to:

$$T_{edge} = 2/\omega_B x[\ \mathrm{Arcsin}[(N+1/2)d-z_0)eF/2|\lambda|\ ] + \mathrm{Arcsin}[(N+1/2)d-z_0)eF/2|\lambda|\ ]] \qquad (V\text{-}26)$$

One notices that the Bloch oscillator centered right on the edge (z_0 = (N+1/2)d) and which does not bounce the -(N+1/2)d other interface has a period which is half of that of the bulk Bloch oscillator. A similar result is obtained for a regular harmonic oscillator bouncing on an infinitely repulsive wall placed at its equilibrium position.

Let us now examine the quantum treatment of eq.(V-15) restricting ourselves to a <u>one band</u> tight binding expansion. The general form of the spectrum can be obtained without any approximation. Suppose that ψ_ν is a solution of eq.(V-15) corresponding to the eigenvalue ε_0. Consider the function $\mathcal{T}_d\,\psi_\nu(z) = \psi_\nu(z + d)$ and apply H on it. We find:

$$H\mathcal{T}_d\,\psi_\nu(z) = (\varepsilon_0\text{-}eFd)\,\mathcal{T}_d\,\psi_\nu(z) \qquad (V\text{-}27)$$

which shows that $\mathcal{T}_d\,\psi_\nu(z)$ is an eigenstate of H corresponding to the energy ε_0-eFd. This procedure can be iterated and so can the application of $\mathcal{T}_d^+$ (= $\mathcal{T}_{-d}$) which translates the energies upward. Finally through the successive translations $\mathcal{T}_{jd}$, j a relative integer, one generates the ladder:

$$\varepsilon_\nu = \varepsilon_0 + \nu eFd\ ,\quad \nu \text{ a relative integer} \qquad (V\text{-}28)$$

Since we have restricted our analysis to a <u>one band</u> tight binding description of the problem there are as many available states as periods in the superlattice (i.e. a countable infinity). Thus, the spectrum given by eq.(V-28) exhausts all the possible states of the biased superlattice and we may conclude that in the one band analysis the Wannier-Stark ladders are evenly spaced. Notice that the one band assumption is here crucial insofar as the unknown ε_0 in eq.(V-28) is necessarily unique. Had we included several bound states per well or, a fortiori, the continuum states, it would have been impossible to draw any conclusion on the even spacing of the level and, in fact, when several bound states are included in the calculations, the spectrum is unevenly spaced. What remains however is the existence of a periodicity in eFd on the energy scale because eq.(V-27) always holds, but the "elementary cell" of this periodic "lattice" instead

of containing a single eigenvalue contains as many of them as the number of states per period which have been retained. The one band result is called a Wannier-Stark ladder since Wannier first derived it[129,133]. In its derivation, he was able to prove that ε_0 is actually the center of gravity of the band at zero field:

$$\varepsilon_0 = d/2\pi \int_{BZ} \varepsilon_1(q)dq \qquad (V\text{-}29)$$

which coincides with E_1 in the simplest tight binding scheme. The spacing between two consecutive eigenvalues is $\hbar\omega_B$ as one could have anticipated from the semiclassical result.

The Wannier-Stark spectrum recalls in many respects the harmonic oscillator one. There exists several differences however. Firstly, the Wannier-Stark spectrum has no ground state, which implies that the usual rules on the nodes of the eigenfunctions do not apply. In fact each eigenstate of the Wannier-Stark problem has an infinite number of nodes and the ψ_ν 's are all but the same wavefunction whose argument is translated by an integer times d (since $T_{jd}\,\psi_\nu = \psi_{\nu-j}$) when going from one state to the other. The equivalent of the raising (c^+) and lowering operator (c) of the harmonic oscillator are the translation operators T_d^+ and T_d respectively. However, T_d and T_d^+ commute while c and c^+ do not. This has some important implications when considering the perturbation of a Wannier-Stark ladder by a harmonically varying electric field, i.e. when one addresses the question of light absorption or emission by an electron moving in a linearly biased superlattice. We shall return to this point later on.

To know more about the actual shape of the ψ_ν's we expand the solutions of H on the basis spanned by the $\phi_{loc}(z\text{-}nd)$ which are the isolated quantum well eigenstates (confinement energy E_1) centered at z = nd:

$$\psi_\nu = \sum_n c_{n\nu}\,\phi_{loc}(z\text{-}nd) \qquad (V\text{-}30)$$

We assume the ϕ's are orthonormalized (a convenient oversimplification), neglect couplings between all the neighbours but the nearest and absorb the shift integral into a redefinition of E_1 to finally end up with the secular equation:

$$c_{nv}(E_1-\varepsilon_v +eFnd) - |\lambda|(c_{n+1v} + c_{n-1v}) = 0 \qquad (V\text{-}31)$$

where the identification of the $< \phi_n | eFz | \phi_m >$ matrix elements to $eFnd\delta_{n,m}$ has been used. One recognizes in eq.(V-31) the recursion relations of the Bessel functions. If the superlattice is infinite the c_{nv}'s should not blow up , which implies that the divergent Bessel functions (I_n) should be eliminated . This leaves us with:

$$c_{nv} = J_{v-n}(-2/f) \qquad (V\text{-}32)$$

$$\varepsilon_v = E_1 + veFd \qquad (V\text{-}33)$$

where f is the dimensionless strength of the electric field:

$$f = eFd/|\lambda| = 4eFd/\Delta_1 \qquad (V\text{-}34)$$

In finite superlattices one should take the c_n's as linear combinations of the J_n's and I_n's and determine the eigenenergies by writing appropriate boundary conditions at the superlattice edges (see Saitoh[141] for a more complete account of edge effects on Wannier-Stark ladders).

Equations (V-32-34) call for several remarks. Firstly, the one band tight binding model provides a universal description of the electric field effects on a superlattice: one only has to scale eFd and $\varepsilon_v - E_1$ to the bandwidth . This scaling allows us to readily understand why the observation of the Wannier-Stark quantization is far more easy to observe in superlattices than in the bulk materials: a typical bandwith in a bulk crystal is 2eV corresponding to a lattice periodicity of 6Å while the corresponding Δ_1 and d are typically 70 meV and 60Å in a superlattice. Assuming an electric field strength of 10^5 V/cm, we get $f_{bulk} \cong 0.012$ and $f_{sl} \cong 3.43$. In other words, the electric field has a small effect in a bulk crystal compared to that produced by the periodic potential while in a superlattice the two effects are comparable. Secondly, the replacement of the extended minibands spectrum by a set of discrete localized levels as evidenced by eqs.(V-33) calls for a physical interpretation. This is the field-induced turning off of the tunnel effect between consecutive wells which is at the heart of the Wannier-Stark quantization and which again explains why the semiconductor superlattices are ideal candidates for its

observation. Consider the biased superlattice (or bulk material) as a collection of localized potential wells whose bound states are misaligned by the electric field and which are nearest neighbour coupled with an interaction strength $-|\lambda|$. By extension of the familiar H_2^+ molecular ion or the double well (section(V.2)) problems, we know that the tunnel coupling between the wells 0 and n will remain operative if the misalignement between the two levels neFd remains smaller than $2|\lambda|$ (see fig.(53))[130]. This means that the number of sites visited by an eigenstate ψ_ν on each side of the ν^{th} site is $2|\lambda|/eFd = 2/f$. Thus, for a typical bulk material, a Wannier-Stark state extends over 2x170 periods while for the same field strength ψ_ν hardly extends beyond the ν^{th} site in a superlattice. This is because the superlattice periods are larger that the minibands are narrower and that the misalignement of consecutive energy levels are bigger than the corresponding quantities in bulk materials that the tunnel coupling between the wells of the superlattice can be so effectively turned off. An extra benefit is gained by the 10 fold increase between consecutive eigenstates of the ladder, making the ratio $eFd/(h/\tau)$ ($= \omega_B\tau$, where τ is scattering time) 10 times longer in a superlattice than in a bulk material if the τ's are identical. Notice finally that the argument on the number of sites visited by an electron in any of the Wannier-Stark state on each side of the ν^{th} site leads to a result (2/f) which exactly coincides with the amplitude of the Bloch oscillator.

A more quantitative assessement of the spatial localization of the ψ_ν's is obtained by computing $P_{n\nu}$, the modulus squared of the projection of ψ_ν onto the localized wavefunction $\phi_{loc}(z\text{-}nd)$. from eq.(V-30) we see that $P_{n\nu}$ is equal to $(c_{n\nu})^2$. Figure(54) shows a plot of $P_{n\nu}$ versus $|\nu\text{-}n|$ for different values of f. The increasing localization around the ν^{th} period when f increases is evident. This localization is very strong (faster than exponential) since $J_p^2(x) \cong x^{2p}/(p!)^2$ if x is small.

Another striking property of the Wannier-Stark states (when compared with our intuitive expectation) is the even probability distribution of the ψ_ν around the ν^{th} period (since $J_{n-\nu}(x) = (-1)^{n-\nu} J_{\nu-n}(x)$). In the one band approximation, there is as much probability for a Wannier-Stark state to be found in regions of lower than in regions of higher electrostatic potential energy, while one might have expected a piling up of the eigenstates where this energy is the lower. Such a piling up for instance occurs for the lowest state of a biased single quantum well, but the comparison between the two results is , we believe, not pertinent. A better one is made if one compares the spatial distribution of

the ν^{th} Wannier-Stark state around the ν^{th} period with that of the second level of a biased single quantum well which binds at least three levels at zero field. In the latter structure, the E_2 level shift (and thus the spatial polarization) depends sensitively on the energy separation E_3-E_2 and E_2-E_1 at zero field: the lower level pushes E_2 upward while E_3 counterbalances this trend. In some occasion, there is nearly a cancellation of these two effects, which leads to a small shift of the E_2 state (ideally a vanishing one). The E_2 eigenfunction remains then nearly unpolarized, like at zero field, and thus displays an almost equidistribution over the regions of higher and lower electrostatic potential energy. The exactly even spatial distribution of the Wannier-Stark states around their center appears in the light of the previous discussion as resulting from the peculiar situation where equidistant levels (the diagonal terms E_1+neFd in eq.(V-31)) are symmetrically coupled to their nearest neighbours.

To complete our survey of the one band analysis of the Wannier-Stark ladders let us summarize the comparison between the quantum and the semi-classical approaches. We have already mentionned that the semi-classical motion occurs with an angular frequency ω_B which is exactly that expected from the quantum spacing $\hbar\omega_B$. Moreover, we found that a rough evaluation of the spatial extent of a quantum eigenstate is just equal to the amplitude of the Bloch oscillator. This agreement can be further quantified by calculating the root mean square deviation Δ_z of the particle position around its equilibrium position:

$$\Delta_z = \left[<(z-z_0)^2> - <z-z_0>^2\right]^{1/2} \qquad \text{(V-35)}$$

where the symbols <..> either denote quantum averages over ψ_ν (with $z_0 = \nu d$) or over the period $2\pi/\omega_B$ of the semi-classical motion. We find:

$$[\Delta_z]_{Bloch} = 2d\sqrt{2}/f \qquad \text{(V-36)}$$

$$[\Delta_z]_\nu = < \phi_0 \mid z^2 \mid \phi_0> + 2d\sqrt{2}/f \qquad \text{(V-37)}$$

Both expressions are nearly identical in the limit of small f (where one indeed expects the semi-classical analysis to be the more valid). For strong fields the field dependent uncertainty decrease in both cases as both the semi-classical and quantum motions become increasingly

restricted. This shrinking can reach a complete collapse in the case of the Bloch oscillator, since both the position and velocity of the Bloch oscillator can be defined with an arbitrary accuracy whereas, in the quantum case, there always remains a residual uncertainty $< \phi_0 \mid z^2 \mid \phi_0 >$ associated with the finite extension of the isolated well eigenstates in the well and barrier layers.

An even more demanding comparison between the two descriptions is obtained by plotting the integrated probability of finding the particle in the j^{th} cell versus j when the oscillator is centered at $z=\nu d$. The classical probability is equal to:

$$P_{j\nu} = 2 \int_{j^{th}cell} dz/|v_z| \qquad (V\text{-}38)$$

if the Bloch oscillator visits the j^{th} cell and $P_j = 0$ elsewhere. The quantum probability is equal to:

$$P_{j\nu} = \int_{j^{th}cell} dz \; |\psi_\nu|^2 \qquad (V\text{-}39)$$

$$= \sum_{ll'} c_{l\nu} \, c_{l'\nu} \int_{j^{th}cell} \phi_{loc}(z-ld) \; \phi_{loc}(z-l'd \;) dz \qquad (V\text{-}40)$$

If the "atomic" wavefunction $\phi_{loc}(z-ld)$ is well localized in the well centered at z=ld, one gets to a good approximation:

$$P_{j\nu} = |c_{j\nu}|^2 = J_{\nu-j}^2(2/f) \qquad (V\text{-}41)$$

The comparison between the classical and quantum $P_{j\nu}$ is shown in fig.(55) for a small value of the reduced electric field. The agreement between both descriptions is excellent and recalls the well known outcome of a similar comparison for a regular harmonic oscillator.

We have previously mentionned that the Wannier-Stark ladder has no ground state and that T_d^+ and T_d , the equivalent of the harmonic oscillators raising and lowering operators, commute. These two properties lead to an interesting consequence with respect to the response of the Wannier-Stark state to a sinusoidally varying electric field (parallel to the static one). Let the electromagnetic (e.m.) perturbation be described by $eF_{em}z\cos(\omega t)$. If F_{em} is small one can investigate by perturbation the transition rate that an electron in the ν^{th} state makes a

transition to the μ^{th} one. This rate is proportional to $|\langle\nu|z|\mu\rangle|^2$. By using the tight binding expansion (eq.(V-30)) we get:

$$\langle\nu|z|\mu\rangle = \sum_{ll'} c_{l\nu}\, c_{l'\mu} \langle\phi_{loc}(z-ld)\ |z|\ \phi_{loc}(z-l'd)\rangle \qquad (V-42)$$

By writing that $z = (z+ld)-ld$ and by neglecting any integral of the form $\langle\phi_{ld}\,|\,z-ld\,|\,\phi_{l'd}\rangle$ one finally gets:

$$\langle\nu|z|\mu\rangle = \nu d\delta_{\nu,\,\mu} + (d/f)\delta_{\nu,\,\mu\pm1} \qquad (V-43)$$

The diagonal term is of no relevance here since it leads to no absorption or emission of energy by the electron. The off-diagonal term displays the expected shape. Namely, a given Wannier-Stark state is coupled by the e.m. wave to its nearest neighbour. The key point is that the coupling is ν-independent, a feature clearly associated with the fact that all the Wannier-Stark states are characterized by wavefunctions which are isomorphical. If the transitions rates (α) between ν and $\nu\pm1$ are the same, it is not very difficult to show that no net energy is absorbed by the electron due to its interaction with the oscillating electric field[150]. Let f_ν be the (arbitrary) distribution function of the ν^{th} state. The net power absorbed due to the $\nu \rightarrow \nu\pm1$ transitions is $h\omega\alpha\,[f_\nu(1-f_{\nu+1}) + f_{\nu-1}(1-f_\nu) - f_\nu(1-f_{\nu-1}) - f_{\nu+1}(1-f_\nu)]$. This is equal to $h\omega\alpha\,[f_{\nu-1} - f_{\nu+1}]$, i.e. does not depend on f_ν. Instead of considering only the $\nu \rightarrow \nu\pm1$ transitions, one may calculate the net power absorbed due to all the transitions between the states -N, -(N-1),..., N-1, N and find that it is equal to $h\omega\,\alpha\,[f_{-N} - f_N]$. Thus, there is no bulk absorption. The only possible absorption inside a Wannier-Stark ladder is therefore due to edge effects, i.e. to the fact that any real superlattice is finite. Notice that we have neglected the spontaneous emission in the previous analysis. Had we considered the net power absorbed by a regular harmonic oscillator (say a ladder of Landau levels) that the results would have been entirely different. The transition rates $n\rightarrow n+1$ (n-1) would have been proportional to n+1 (n), where n is the Landau level index, and the net power absorbed by the electron due to the $n\rightarrow n\pm1$ transitions would have been proportional to $[(n+1)(f_n - f_{n+1}) + n(f_{n-1} - f_n)]$. The total power absorbed due to all the possible transitions would be proportional to $\Sigma_n(n+1-n)f_n$, i.e. to the concentration of electrons as it should for a bulk effect.

The Wannier-Stark states are thus of little interest for the intraband transitions. They display however rich electro-optical properties which are associated with interband transitions, i.e. to transitions between the valence and conduction ladders. It is not the purpose of the present review to give a detailed account of the optical properties of the Wannier-Stark states (for recent reviews see e.g. (151). Let us only sketch here the salient features.

Consider the possible optical interband transitions in a finite but thick superlattice. The electromagnetic wave is assumed to propagate along the growth axis. The in-plane wavevector has to be conserved for allowed optical transitions in the dipole approximation. If there is no electric field the superlattice wavevector q is conserved as well. If the superlattice is biased, the electrostatic potential breaks the q conservation rule, but we have seen that the superlattice minibands are destroyed and replaced by the Wannier-Stark ladders. For single, parabolic and non degenerate conduction and valence bands, the optical matrix elements involving the coupling between the light and the electron breaks into:

$$M_{cv} = \langle u^c \mid \varepsilon.\mathbf{p} \mid u^v \rangle \langle \psi^{(c)} \mid \psi^{(v)} \rangle \qquad (V\text{-}44)$$

where u^c (u^v) is the periodic part of the conduction (valence) zone center Bloch function, ε is the light polarization vector and $\psi^{(c)}$, $\psi^{(v)}$ are the envelope wavefunctions of the conduction and valence subbands, in our case the Wannier-Stark states $\psi_\nu^{(c)}$, $\psi_\mu^{(v)}$. Notice that although both the valence and conduction ladders are evenly spaced by the same eFd and parallel, the eigenstates $\psi_\nu^{(c)}$, $\psi_\nu^{(v)}$ are not the same, for their projection on the "atomic" wavefunctions $\phi_{loc}^{(c)}(z\text{-}nd)$, $\phi_{loc}^{(v)}(z\text{-}nd)$, namely $J_{\nu\text{-}n}(-2/f_c)$, $J_{\nu\text{-}n}(2/f_v)$, are different due to the different conduction and valence subband widths. The overlap integrals $\langle \psi^{(c)} \mid \psi^{(v)} \rangle$ are thus, in general, non vanishing and all the possible transitions between ν and μ become allowed. This result, again, contrasts with the case of the magneto-absorption (i.e. the interband transitions between Landau levels) where, in spite of different ladder spacings ($\hbar\omega_c$ and $\hbar\omega_v$) the conduction and valence eigenstates are the same for a given n, which leads to the selection rule on the envelope functions $\Delta n = 0$.

It is not very difficult to calculate the transition rates for $|v, \mu\rangle \rightarrow |c, \nu\rangle$ transitions, to integrate over $\mathbf{k}_\perp$, taking into account its conservation in the optical process and to finally end up with an

absorption coefficient which, for a type I superlattice, in the limit of a thick sample is given by[125]:

$$\alpha(\omega) = (2N+1)\alpha_0 \Sigma_p J_p^2(2/f_{cv})Y[h\omega-(\varepsilon_g+E_1+HH_1+peFd)] \qquad (V\text{-}45)$$

where 2N+1 is the (large) number of periods in the superlattice, Y(x) the step function, ε_g the bandgap of the well-acting material, E_1 and HH_1 the confinement energies of the ground electron and hole states in the quantum wells when they are isolated, p a relative integer ($-N \leq p \leq +N$) and f_{cv} the dimensionless electric field strength:

$$f_{cv} = eFd/(|\lambda_c| + \lambda_v) \qquad (V\text{-}46)$$

Finally, α_0 is the absorption coefficient related to the $HH_1 \rightarrow E_1$ optical transition in the isolated quantum well ($\alpha_0 \cong 0.6\%$ in III-V quantum wells). We see that the absorption coefficient is just the sum of staircase absorption edges taking place at the energies $\varepsilon_g + E_1 + HH_1 + peFd$. These staircases have a simple physical explanation: they are associated with the oblique transitions in real space which promote an electron in the 0^{th} valence Wannier-Stark state to the p^{th} conduction one. These oblique transitions are symmetrically placed on the energy scale with respect to the p=0 vertical transition. There is therefore no absorption edge for the band-to-band transitions (if $NeFd > \varepsilon_g + E_1 + HH_1$). However, the oscillator strength of the oblique transitions sharply drop with p, to such an extent that they quickly become unmeasurably small. We illustrate these considerations in fig.(56) where the absorption coefficient of a 41 periods superlattice is plotted versus the reduced photon energy ε ($\varepsilon = [h\omega-(\varepsilon_g+E_1+HH_1)]/(|\lambda_c| + \lambda_v)$) for several field strengths f_{cv}. At zero field the unperturbed superlattice absorption coefficient is drawn and displays the well-known Arccosine shape. When f_{cv} increases steps corresponding to the oblique ($p\neq0$) and vertical (p=0) transitions develop. It is seen that their amplitudes are not monotonic functions of f_{cv} (because J_p^2 has an infinite number of nodes). However, when $f_{cv} > f_p$, where $2/f_p$ is the smaller zero of J_p^2, the p^{th} oblique transition fades away. For $f_{cv} > 4$ (which corresponds to a potential energy drop over a period equal to the sum of the conduction and valence subband widths), one is left with a dominant p = 0 vertical step (nearly 90% of the total absorption coefficient) and two small p = ±1 steps, evenly sharing the

remaining 10% of the absorption. There is therefore an effective blue shift of the band-to-band absorption edge. This blue shift can be quite large since $1/2(\Delta_c+\Delta_v)$ can easily reach 30 meV. Notice that when the blue shift is significant, the well and barrier thicknesses are usually small ($\cong$ 30Å), which implies that the intra-well Stark shift (E_{SQW}) discussed in section (V.2) is small ($\cong$ 1-2 meV). On the other hand, the excitonic effects (to be discussed in section VII) become larger with increasing f_{cv} because the structure continuously evolves from a quasi three dimensional material (f_{cv} = 0) to a quasi bi dimensional material ($f_{cv} \geq 4$), which enhances the exciton binding energy. Thus, the measurable blue shift Δ_{BS} is limited to:

$$\Delta_{BS} = 1/2(\Delta_c+\Delta_v) - (R^*_{QW} - R^*_{SL}) - E_{SQW} \qquad (V\text{-}47)$$

where $R^*_{QW} - R^*_{SL}$ is the increase of the exciton binding energy when going from the coupled to the electric field-isolated quantum well situations. We show in figs.(57-59) an estimate of the periods where a useful blue shift can be obtained in three different superlattice systems assuming equal well and barrier thicknesses. The criteria used to define the rectangles in figs.(57-59) are that $1/2\Delta_c$ should be larger than 10 meV and that the electric field required to achieve an almost complete Wannier-Stark localization (f = 4) should be smaller than 10^5V/cm. It is seen that for the three systems a period d = 70 Å , which is not exceedingly demanding from the growth point of view, fulfills both criteria. Figure (60) illustrates the experimental confirmation of the blue shift in a (Ga,In)As-(Ga,Al,In)As superlattice[147] and the significant potentialities of this effect for electro-modulation . Figure (61) shows a "fan" diagram (transition energies versus electric field strength) showing the field dependences of the vertical and oblique transitions in a GaAs-(Ga,Al)As superlattice. Oblique transitions from p=-5 up to p = +3 have been observed, which demonstrates both the relevance of the Wannier-Stark description of a biased superlattice and the fact that the coherence of the conduction states extends at least up to 7 periods (the hole states are quickly field-localized in a given period and, actually, act as markers[153] of the conduction envelope functions).

V.4.b. *Multiband effects on the Wannier-Stark quantization*

The previous paragraph has been devoted to a one band tight binding analysis of the Wannier-Stark quantization. In reality, any bulk or

superlattice band structure displays an infinite number of bands. Let n be the subband index of a superlattice miniband centered at E_n. The zeroth order of approximation consists of constructing a Wannier-Stark ladder attached to each subband:

$$\varepsilon_{n\nu} = \varepsilon_{n0} + \nu eFd \text{ , } \nu \text{ a relative integer} \qquad \text{(V-48)}$$

For discrete values of the field there will exist crossings between $\varepsilon_{n\nu}$ and $\varepsilon_{m\mu}$ ($edF_{\mu\nu} = (\varepsilon_{n0}-\varepsilon_{m0})/(\mu-\nu)$). In reality these crossings are replaced by anticrossings since there is no reason why the matrix elements $< \phi_{loc}^{(n)}(z\text{-}id) \mid eFz \mid \phi_{loc}^{(m)}(z\text{-}jd) >$ should all be zero if $m \neq n$. When considering the ladders whose energy corresponds to the continuum the index n or m becomes continuous and thus there exists a broadening of the $|n\nu>$ Wannier-Stark state due to its interaction with the $|m\mu>$ continuum. These interactions have long cast doubts[134-141] on the very existence of the Wannier-Stark ladders, for it may have happened that the escape could have been faster than the Bloch period T_B, invalidating Wannier's approach. It took some time to formally establish that these effects were in practice small, a feature which recalls the findings in the problem of the intra-well Stark effect (section (V.2)) were one also deals with virtual bound states but where many physical quantities are accurately calculated by models which neglect the interaction with the continuum.

If one thus forget about finite lifetime effects, there are still possibilities of interactions between the ladders attached to different subbands generated by the hybridization of different quantum well bound states. In the vicinity of the $F_{\mu\nu}$'s defined above, the eigenstates which were field-localized in the one band approximation delocalize again. This delocalization, similar to the one described in section (V.3) for double wells, is very important for the carrier relaxation and transport along the growth axis. Notice however that its spatial extent is limited: if only nearest neighbour couplings are significant the larger achievable delocalization, out of completely localized states at the zeroth order of approximation, takes place over two superlattice periods at the maximum of the anticrossing between the two interacting ladders.

The reasoning we made in section (V.4.a) about the linear variation of the Wannier-Stark states with F is no longer operative when several bound states per period are admixed by the field. Instead of dealing with a single ε_0 appearing as an additive constant to all the energy levels of a ladder, and thus liable to be absorbed in a redefinition of the zero of

energy or to be evaluated by some direct calculations (e.g. ε_0 = center of gravity of the miniband), there are as many ε_{n0} as bound states per period. They cannot be all eliminated. Moreover, the previous reasoning on the T_d (eq.(V-27)) is unable to tell us a priori if the ε_{n0} are field dependent or not, which precludes us to assert that the eigenstates vary linearly with F in the multiband situation. In fact they do not, as shown by the numerical diagonalizations of the superlattice hamiltonian. What remains true however, is the fact that the sequence $\varepsilon_\nu^{(n)}$, where n =1,2,..,M labels the various bound states per period, repeats itself periodically on the energy scale and that the wavefunctions $\psi_\nu^{(n)}(z)$ generate all the eigenfunctions of the problem by successive applications of T_d or T^+_d. Figure(62) shows the calculated eigenstates of a 11 period (100Å-20Å) GaAs-$Ga_{0.7}Al_{0.3}As$ biased superlattice versus the electric field strength. The well thickness is such that two states are bound at zero field. The eFz term has been diagonalized within the basis spaned by the 2x11 bound states at zero field. At zero electric field one sees clearly two minibands centered around 30 meV and 117 meV respectively. Since the superlattice is finite, each of the subband continuum actually gives rise to 11 levels. At non vanishing F the actual spectrum is derived from the two interpenetrating Wannier-Stark ladders $E_1+\nu d$, $E_2+\mu d$ ($-5\leq \nu, \mu \leq 5$) attached to the two zero-field subbands. There exist two kinds of departures to the zeroth order spectra. The first kind is an edge effect: since the superlattice is finite and that there exist 2x11 non degenerate bound levels at zero field, the small field behaviour (here $F \leq$ 1kV/cm) should be a quadratic regime analogous to the intra-well Stark effect described in section (V.2). Because the "equivalent quantum well" is very thick the non degenerate perturbation approach which describes the quadratic Stark shift quickly becomes invalid and the levels start varying linearly with F . The departure from the linear behaviour is the smaller for the central level and the larger for the ±5 levels which are the more sensitive to the edges (see section (V.4.a) for the related "edge interacting" Bloch oscillators). For field stengths near $F_{\mu\nu}$ there exists a second kind of departures from the 0th order of approximation. They are the field-induced resonant tunnelling effects taking place between the different levels of the two ladders which, in the limit of a strong Wannier-Stark localization, would coincide with the isolated well eigenstates. These effects are the more pronounced when $\mu-\nu$ is the smaller (±1), which happens when $F_{\mu\ \mu\pm1}$ is equal to 80kV/cm. For F > 80kV/cm edge and anticrossing effects become negligible and the regime

of linearly varying levels should, apart from the intra-well Stark effect, be recovered.

When dealing with the Wannier-Stark ladders in the valence band of superlattices, one faces a more difficult numerical problem than met for the conduction ladders. In the latter case we were able, by implicitly neglecting non parabolicity effects, to decouple the z and x,y motions and, thus, to deal only with a one dimensional Schrodinger equation. We have seen in section IV that such a decoupling is impossible for the valence subbands except if the in-plane wavevector $\mathbf{k}_\perp$ vanishes. One has therefore to recourse to numerical diagonalization of the valence hamiltonian in finite structures to find the in-plane dispersion relations of the valence Wannier-Stark ladders[49]. The fact that there exist two categories of hole levels at $\mathbf{k}_\perp=0$ (heavy and light holes), which in the diagonal approximation of the Luttinger hamiltonian display different in-plane effective masses (mass reversal effect), implies that in addition to the regular multiband anticrossing effects taking place at $\mathbf{k}_\perp=0$ (similar to those discussed above for electrons) one has also to expect that there will exist anticrossings occuring at $\mathbf{k}_\perp\neq\mathbf{0}$ which are a consequence of the off diagonal terms of the Luttinger matrix. Despite this very complex situation, the notion of the Wannier-Stark ladder is still relevant for the valence subbands, at least with the generalized meaning specified above for electrons. In fact, let us consider the valence hamiltonian of a biased superlattice and assume again that one can restrict our considerations to the J=3/2 topmost quadruplet. The hamiltonian is now a 4x4 matrix and its eigenstates $\psi(\mathbf{r})$ are 4x1 spinors:

$$\{ \mathbf{T} + \mathbf{1}(V(z)+eFz) \}\, \psi(\mathbf{r}) = \varepsilon\, \psi(\mathbf{r}) \qquad \text{(V-49)}$$

where **1** is the 4x4 identity matrix and **T** the Luttinger kinetic energy term (eq.(II-24)). Since the potential energy depends only on z, $\psi(\mathbf{r})$ factorizes into

$$\psi(\mathbf{r}) = \psi_{\mathbf{k}\perp}(\mathbf{z})\, \exp(i\, \mathbf{k}_\perp.\mathbf{r}_\perp)\, /\sqrt{S} \qquad \text{(V-50)}$$

From now on we drop the $\mathbf{r}_\perp = (x,y)$ dependence and focus on $\psi_{\mathbf{k}\perp}(\mathbf{z})$ which is implicitly $\mathbf{k}_\perp$-dependent since it is the solution of a $\mathbf{k}_\perp$-dependent hamiltonian.

Suppose that $\psi_{\mathbf{k}\perp}(\mathbf{z})$ is an eigenstate of eq.(V-49) corresponding to an energy ε_0. Thus, $\mathcal{T}_d\, \psi_{\mathbf{k}\perp}(\mathbf{z})$ is also an eigenstate corresponding to

ε_0-eFd. There is therefore a Wannier-Stark ladder but, like in the case of conduction ladders with multi subband effects, this does not imply a linear variation of the eigenenergies with F. Besides, the ε_0 has not only to be indexed by n, where n=1,2,...,2N and N is the number of interacting hole subbands, but also by $\mathbf{k}_\perp$ since the hamiltonian changes with $\mathbf{k}_\perp$ (and not only by an additive constant). Thus, one can conclude that if one only takes into account the bound hole states, the valence spectrum of a biased infinite superlattice consists of an evenly spaced (by eFd) sequence of groups of states, where each group of states countains twice the number of bound hole states at $\mathbf{k}_\perp$=0. The extra factor of 2 comes from the strong spin-orbit coupling. Only at $\mathbf{k}_\perp$=0 does one recover a twofold degeneracy of each state. As mentioned previously for electrons, the coupling of a ladder attached to a bound state with the continuum states leads to a broadening of the Wannier-Stark states. We shall again assume that this broadening is negligible.

At $k_\perp$=0 the situation is somewhat simpler. The decoupling between the heavy and light hole states (m_J= ±3/2; m_J= ±1/2 respectively) is exact. Also the +3/2 (+1/2) and -3/2 (-1/2) components are uncoupled. Thus, the Wannier-Stark ladders split into two independent categories and each category displays a twofold degeneracy. The situation is much the same as discussed for the conduction states. Notice in particular that there exist anticrossings between the heavy hole Wannier-Stark states attached to different subbands or between the light hole ones. On the other hand exact crossings take place between a heavy hole and a light hole state. This is illustrated in fig.(63) where the field dependence of the valence energy levels is shown for a (50Å-40Å-50Å) GaAs-$Ga_{0.7}Al_{0.3}As$ symmetrical double well. The primed and unprimed levels respectively corresponds to states which are mostly localized on the right hand side and left hand side wells. One notices that the dashed lines (light hole levels) cross the solid lines (heavy hole levels) while two states of the same category anticross (HH_1 and HH'_1 do anticross at F=0 but the anticrossing gap is very small). When $k_\perp \neq 0$ the heavy and light hole levels interact and if F≠0 the twofold degeneracy for a given $k_\perp$ is lifted. We therefore expect that all the crossings will be replaced by anticrossings. This is illustrated in the lower panel of fig.(63) for $k_\perp = 2.5 \times 10^6 cm^{-1}$. Clearly the light hole branches now anticross the heavy hole one and, in fact, the notion of light and heavy hole becomes irrelevant when $k_\perp \neq 0$. As we shall see in section VI the band mixing effects are very

important to understand both qualitatively and quantitatively the assisted hole transfer in biased heterostructures.

In superlattices, one expects the numerical outcomes to agree with the general property about the existence of an evenly spaced sequence of groups of states. Since the numerical diagonalization can only deal with finite superlattices, edge effects may perturb the even spacing. These features are illustrated in figs.(64-66) where we show for F=40kV/cm the in-plane dispersion relations of a 50Å thick GaAs-$Ga_{0.7}Al_{0.3}As$ single quantum well (fig.(64)), of a 3 periods (fig.(65)) and of a 5 periods (fig.(66)) 50Å-50Å GaAs-$Ga_{0.7}Al_{0.3}As$ superlattice. At zero field each isolated well supports two heavy hole states (HH_1,HH_2) and one light hole state (LH_1). At $k_\perp \neq 0$ the levels are labeled according to their $k_\perp=0$ nature and to the well were they are principally localized. One clearly sees the existence of an evenly spaced sequence ($HH_2^{(n)}$,$LH_1^{(n+1)}$,$HH_1^{(n+2)}$) when n, n+1, n+2 are such that they do not correspond to a terminating well of the finite superlattice. Notice that the members of the group of states generating the sequence change with F. In particular, in the limit of a large field the group should only contain levels which all are mainly localized in the same well. In this limit the spectrum of the finite superlattice is just a repetition on the energy scale of that of a biased single well.

An example of the band mixing effects is shown in figs.(67a,b) where the $k_\perp$ dependence of $\sqrt{<J_z^2>}$ is shown for a single 50Å thick GaAs - $Ga_{0.7}Al_{0.3}As$ quantum well (fig.(67a)) and for the group of states genereting a Wannier-Stark ladder in a 50Å-50Å GaAs-$Ga_{0.7}Al_{0.3}As$ superlattice (fig.(67b)). If there were no band mixing effects $\sqrt{<J_z^2>}$ would either be equal to 3/2 (heavy hole state) or 1/2 (light hole state). The departures from these two values arise from the off diagonal and $k_\perp$ dependent terms of the Luttinger matrix. The comparison between fig.(67a) and fig.(67b) allows one to specify if the band mixing is an intra-well effect or arises from the interaction between the heavy and light hole states mainly localized in different wells.

[116] G. Bastard, E.E. Mendez, L.L. Chang and L. Esaki, Phys. Rev. B 28, 3241 (1983).

[117] D.A.B. Miller, D.S. Chemla, T.C. Damen, A.C. Gossard, W. Wiegmann, T.H. Wood and C.A. Burrus, Phys. Rev. Lett. 53, 2173 (1984) and Phys. Rev. B 32, 1043 (1985).

[118] D.A.B. Miller, D.S. Chemla and S. Schmitt-Rink, Phys. Rev. B 33, 6976 (1986).

[119] D.A.B. Miller, J.S. Weiner and D.S. Chemla, IEEE J. Quantum Electron. QE22, 1816 (1986).

[120] K. Wakita, Y. Kawamura, Y. Yoshikuni, H. Aoahi and S. Uehara, IEEE J. Quantum Electron. QE22, 1831 (1986).

[121] D.A.B. Miller, D.S. Chemla, T.C. Damen, A.C. Gossard, W. Wiegmann, T.H. Wood and C.A. Burrus, Appl. Phys. Lett. 45, 13 (1984).

[122] J.A. Brum and G. Bastard, Phys. Rev. B 31, 3893 (1985).

[123] E.J. Austin and M. Jaros, Appl. Phys. Lett. 47, 274 (1985).

[124] E.E. Mendez, G. Bastard, L.L. Chang, L. Esaki, H. Morkoc and R. Fisher, Phys. Rev. B 26, 7101 (1982).

[125] J. Bleuse, G. Bastard and P. Voisin, Phys. Rev. Lett. 60, 220 (1988).

[126] E.E. Mendez, F. Agullo-Rueda and J.M. Hong, Phys. Rev. Lett. 60, 2426 (1988).

[127] L. Vina, E.E. Mendez, W. Wang, L.L. Chang and L. Esaki, J. Phys. C Solid State Phys. 20, 2803 (1987).

[128] G. Bastard, C. Delalande, R. Ferreira and H.W. Liu, J. of Luminescence 44, 247 (1990).

[129] G.H. Wannier "Elements of Solid State Theory" (Cambridge University Press, Cambridge 1959).

[130] A similar localization occurs due to barrier height or layer thickness fluctuations ; see e.g. : R. Lang and K. Nishi, Appl. Phys. Lett. 45, 98 (1984) for double quantum wells. For disordered-induced localization in superlattices see references [79-85].

[131] R.F. Kazarinov and R.A. Suris. Fiz. Tekl. Poluprovodn. 6, 148 (1972) [Sov. Phys. -Semicond. 6, 120 (1972)].

[132] F. Bloch, Z. für Physik 52, 555 (1928).

[133] G.H. Wannier, Rev. Mod. Phys. 34, 645 (1962).

[134] J. Zak, Phys. Rev. Lett. 20, 1477 (1968) and Solid State Physics, volume 27, p. 1 (Academic Press, New York, 1972).

[135] J.B. Krieger and G.J. Iafrate, Phys. Rev. B 33, 5494 (1986).

[136] D. Emin and C.F. Hart, Phys. Rev. B 36, 7353 (1987).

[137] Qian Niu, Phys. Rev. B 40, 3625 (1989).

[138] J. Callaway, Phys. Rev. 130, 549 (1963).

[139] M. Luban and J.H. Luscombe, Phys. Rev. B 34, 3674 (1986).

[140] F. Bentosela, V. Grecchi and F. Zironi, Phys. Rev. Lett. 50, 84 (1983) and J. Phys. C 15, 7119 (1982).

[141] M.J. Saitoh, J. Phys. C 5, 914 (1972).

[142] R.W. Koss and L.M. Lambert, Phys. Rev. B 5, 1479 (1972).

[143] W. Franz, Z. Naturforsch. Teil A13, 484 (1958).

[144] L.V. Keldysh, Zh. Eksp. Teor. Fiz. 34, 1138 (1958) ; [Sov. Phys. -JETP 7, 788 (1958)].

[145] P. Voisin "A superlattice optical modulator", french patent (1986).

[146] P. Voisin, J. Bleuse, C. Bouche, S. Gaillard, C. Alibert and A. Regreny, Phys. Rev. Lett. 61, 1639 (1988).

[147] J. Bleuse, P. Voisin, M. Allovon and M. Quillec, Appl. Phys. Lett. 53, 2632 (1988).

[148] I. Bar-Joseph, K.W. Goossen, J.N. Kuo, R.F. Kopf, D.A.B. Miller and D.S. Chemla, Appl. Phys. Lett. 55, 340 (1989).

[149] R. Ferreira and G. Bastard, Phys. Rev. B 38, 8406 (1988).

[150] G.H. Döhler (1988) private communication.

[151] P. Voisin, Surf. Sci. 1990, in press.

[152] F. Agullo-Rueda, E.E. Mendez and M.H. Hong, Phys. Rev. B 40, 1357 (1989).

[153] J. Barreau, K. Khirouni, Do Xuan Than, T. Amand, M. Brousseau, F. Laruelle and B. Etienne, Solid State Commun. (1990) in press.

FIGURE CAPTIONS

Fig.(45) : Two approximate ways to calculate the metastable states of a quantum well tilted by an electric field.

Fig.(46) : Semiclassical estimates of the escape time of an electron (in the E_1 state) a light hole (LH_1 state) and a heavy hole (HH_1 state) out of quantum wells (L = 30 A, 60 A, 90 A) tilted by an electric field. For the electron, light hole or heavy hole the escape time at a given field increases monotonically with L.

Fig.(47) : Calculated envelope functions for electrons (E_1 state) or holes (HH_1 state) in a GaAs-$Ga_{0.7}A\ell_{0.3}As$ quantum well (L = 200 A) for several electric field strengths (in kV/cm).

Fig.(48) : Calculated energy shifts of the conduction and valence levels in a 100 A thick GaAs-$Ga_{0.7}A\ell_{0.3}As$ quantum well versus the electric field strength.

Fig.(49) : Electric field dependence of the fundamental optical transitions in GaAs-Ga(Aℓ)As quantum wells with different thicknesses. Solid : line theory. Symbols : experiments. After reference [127].

Fig.(50) : Calculated Stark shift of the fundamental optical transition (E_1-HH_1) in Ga(In)As-InP and Ga(n)As-Aℓ(In)As quantum wells with different thicknesses.

Fig.(51) : Calculated conduction eigenstates (solid lines) of a biased 100 A-20 A-100 A GaAs-$Ga_{0.7}A\ell_{0.3}As$ double quantum well versus the electric field strength. The dashed lines are the strong field asymptotes of the decoupled E_1 and E_2 levels in each isolated wells.

Fig.(52a) : Position dependence of the envelope function of the first eigenstate in a 100 A-20 A-100 A GaAs-$Ga_{0.7}A\ell_{0.3}As$ biased

double quantum wells at four different electric field strengths : F=0, 60 kV/cm, 90 kV/cm, 120 kV/cm.

Fig.(52b) : Position dependence of the envelope function of the second eigenstate in a 100 A-20 A-100 A GaAs-$Ga_{0.7}A\ell_{0.3}As$ biased double quantum wells at four different electric field strengths : F=0, 60 kV/cm, 90 kV/cm, 120 kV/cm.

Fig.(52c) : Position dependence of the envelope function of the third eigenstate in a 100 A-20 A-100 A GaAs-$Ga_{0.7}A\ell_{0.3}As$ biased double quantum wells at four different electric field strengths : F=0, 60 kV/cm, 90 kV/cm, 120 kV/cm.

Fig.(52d) : Position dependence of the envelope function of the fourth eigenstate in a 100 A-20 A-100 A GaAs-$Ga_{0.7}A\ell_{0.3}As$ biased double quantum wells at four different electric field strengths : F=0, 60 kV/cm, 90 kV/cm, 120 kV/cm.

Fig.(53) : Conduction band edge profile of a portion of a biased superlattice. Each eigenstate is coupled to its nearest neighbour (interaction strength λ). The delocalization of a particular eigenstate centered at a given site (say 0) is over all the sites whose shaded bands overlap that centered at the 0^{th} site. The eigenstate centered at the 0^{th} site will not extend to the site n=4.

Fig.(54) : Spatial localization of the ν^{th} Wannier Stark state around the ν^{th} site for different reduced field strengths.

Fig.(55) : Comparison between the semiclassical (solid line) and quantum (circles) probabilities of finding the electron in the ν^{th} Wannier Stark state at a given site. f=0.1.

Fig.(56) : Calculated band-to-band absorption lineshape of an infinite superlattice (f=0) and of 41 periods superlattice ($f\neq0$). For f=4 the absorption edge practically reduces to two small steps ($\pm$ 1 oblique transitions) and a large one located at the edge of the isolated quantum well.

Fig.(57) : The critical field needed to achieve the condition f=4 (F_c, left scale) and the maximum blue shift of the E_1 conduction states ($\frac{1}{2}\Delta_{c1}$, right scale) are plotted versus the superlattice period d in GaAs-$Ga_{0.7}A\ell_{0.3}As$ superlattices with equal layer thicknesses. The rectangle defines the area where $F_c < 10^5$ V/cm and $\frac{1}{2}\Delta_{c1} > 10$ meV.

Fig.(58) : Same as fig.(57) but for $Ga_{0.47}A\ell_{0.53}As$-InP superlattices.

Fig.(59) : Same as fig.(57) but for $Ga_{0.47}In_{0.53}As$-$A\ell_{0.48}In_{0.52}As$ superlattices.

Fig.(60) : Measured absorption lineshape versus photon energy at two voltages in a 39 Å-46 Å $Ga_{0.47}In_{0.53}As$-(Ga,Aℓ,In)As superlattice (upper scale). Absorption difference versus photon energy (lower scale). Adapted from reference [147].

Fig.(61) : Electric field dependence of interband transitions between Wannier Stark states in a 60 Å period GaAs-$Ga_{0.65}A\ell_{0.35}As$ superlattice. After reference [152].

Fig.(62) : Calculated conduction eigenstates in a 11 wells 100 Å-20 Å GaAs-$Ga_{0.7}A\ell_{0.3}As$ superlattice versus electric field. The numbers -5,-4,... label the 11 E_1-originating quantum states while the numbers -5',-4',... label the 11 E_2-originating ones. The numbers also correspond to the wells where the eigenstates are mainly localized in strong fields.

Fig.(63) : Calculated field dependence of the valence eigenstates of a 50 Å-40 Å-50 Å GaAs-$Ga_{0.7}A\ell_{0.3}As$ biased double quantum well. $k_\perp$=0 : upper pannel. $k_\perp = 2.5\times10^6\ cm^{-1}$: lower pannel.

Fig.(64) : Calculated in-plane dispersion relations of 50 Å thick GaAs-$Ga_{0.7}A\ell_{0.3}As$ biased single quantum well. F=40 kV/cm.

Fig.(65) : Calculated in-plane dispersion relations of 3 wells

50 A-50 A GaAs-$Ga_{0.7}A\ell_{0.3}As$ biased multiple quantum well. F=40 kV/cm.

Fig.(66) : Calculated in-plane dispersion relations of 5 wells 50 A-50 A GaAs-$Ga_{0.7}A\ell_{0.3}As$ biased multiple quantum well. F=40 kV/cm.

Fig.(67a) : The quantity $\sqrt{\langle J_z^2 \rangle}$ is plotted versus $k_\perp$ for the three bound states of a biased GaAs-$Ga_{0.7}A\ell_{0.3}As$ single quantum well. L=50 A, F=40 kV/cm.

Fig.(67b) : The quantity $\sqrt{\langle J_z^2 \rangle}$ is plotted versus $k_\perp$ for the three central states out of the nine eigenstates of a three well 50 A-50 A GaAs-$Ga_{0.7}A\ell_{0.3}As$ biased superlattice. F=40 kV/cm.

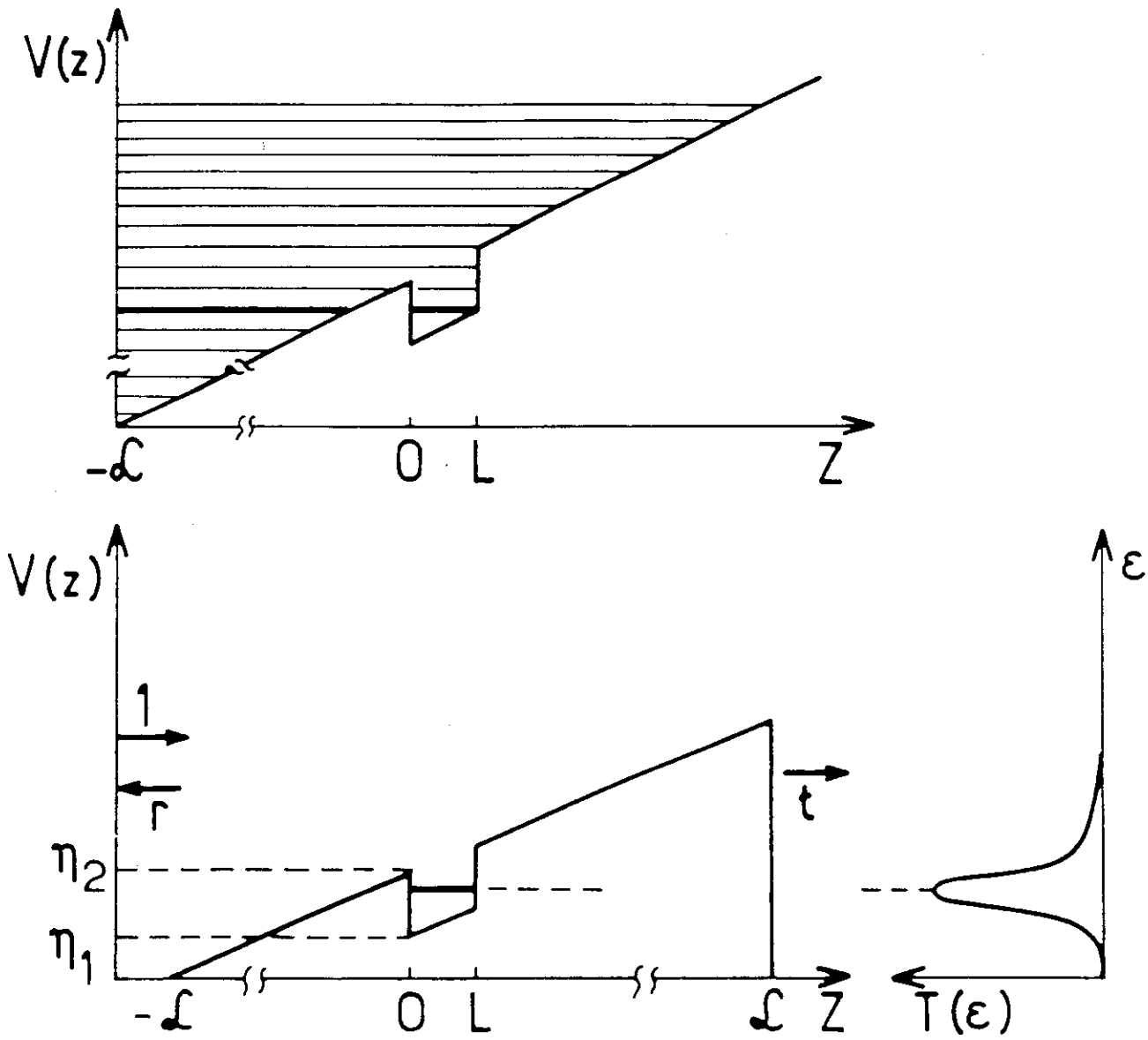

fig. 145)

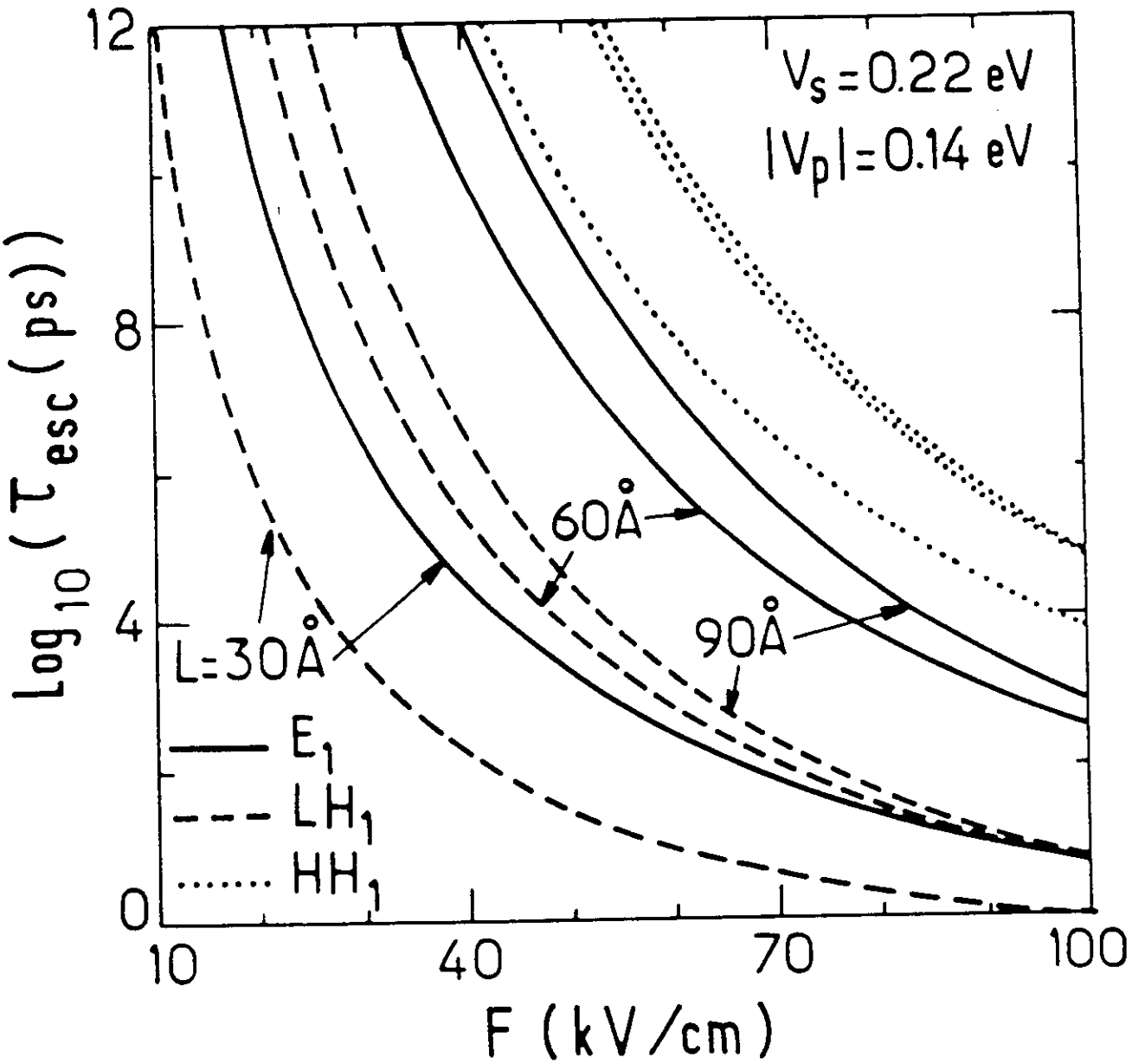
12
8
4
0
10
40
70
100
$V_s = 0.22$ eV
$|V_p| = 0.14$ eV
60Å
90Å
L=30Å
E_1
LH_1
HH_1
$Log_{10}(\tau_{esc}(ps))$
F (kV/cm)

fig. (46)

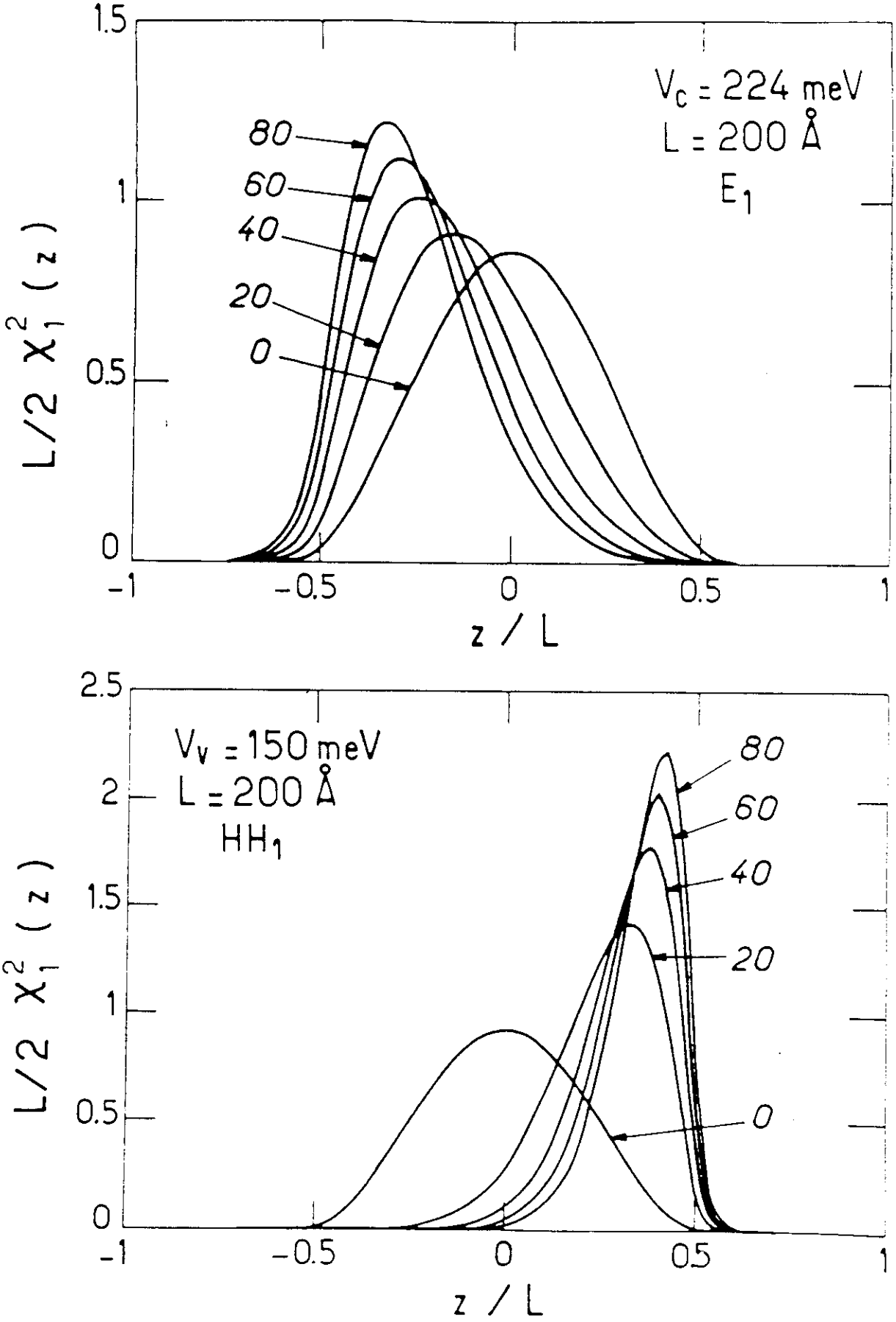
1.5
1
0.5
0
-1
-0.5
0
0.5
1
V_c = 224 meV
L = 200 Å
E_1
80
60
40
20
0
$L/2\ \chi_1^2(z)$
z / L
2.5
2
1.5
1
0.5
0
V_v = 150 meV
L = 200 Å
HH_1
80
60
40
20
0
$L/2\ \chi_1^2(z)$
z / L

fig. (147)

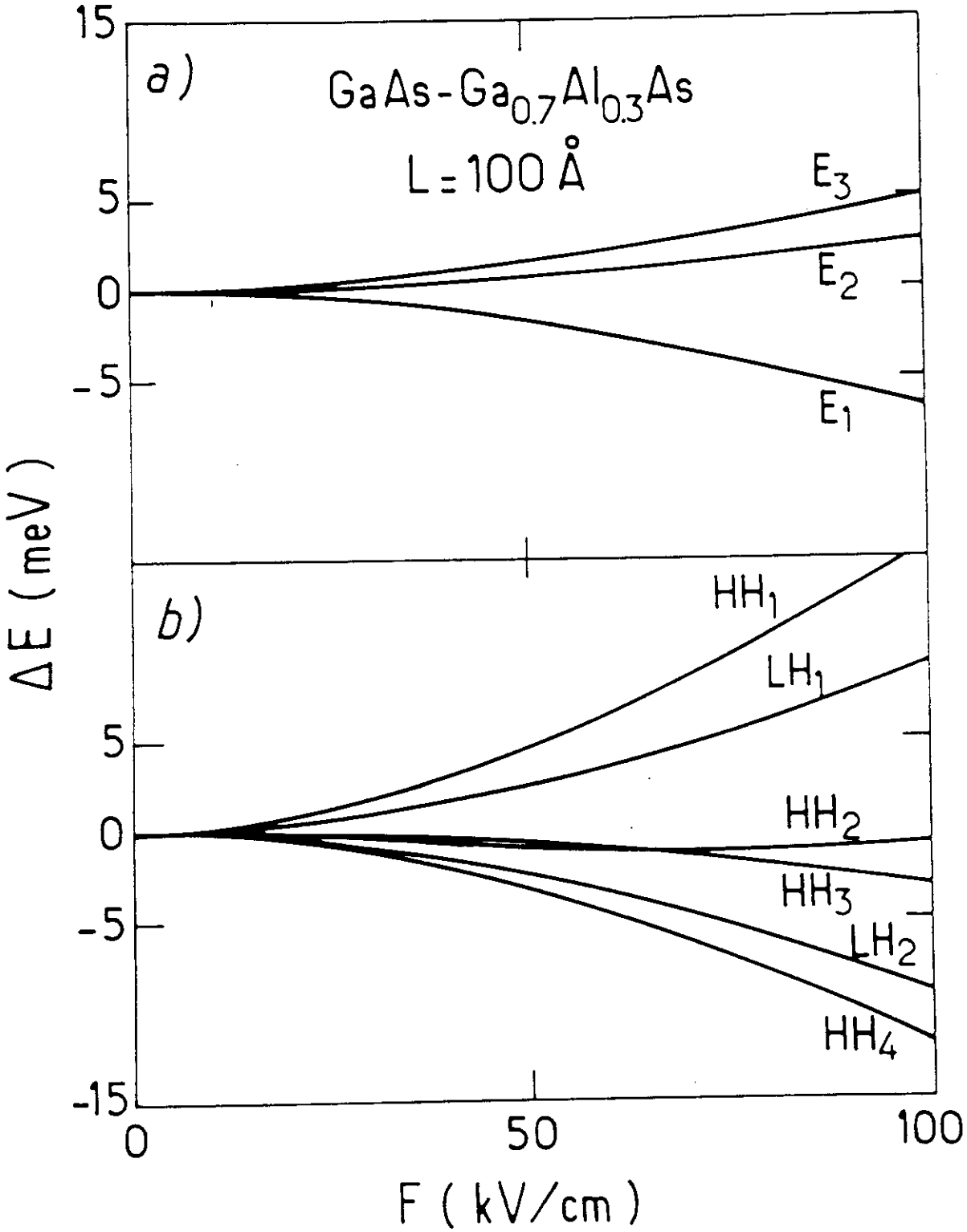
a)
GaAs-Ga0.7Al0.3As
L = 100 Å
E3
E2
E1
b)
HH1
LH1
HH2
HH3
LH2
HH4
15
5
0
-5
-15
0
50
100
ΔE (meV)
F (kV/cm)

fig. 148)

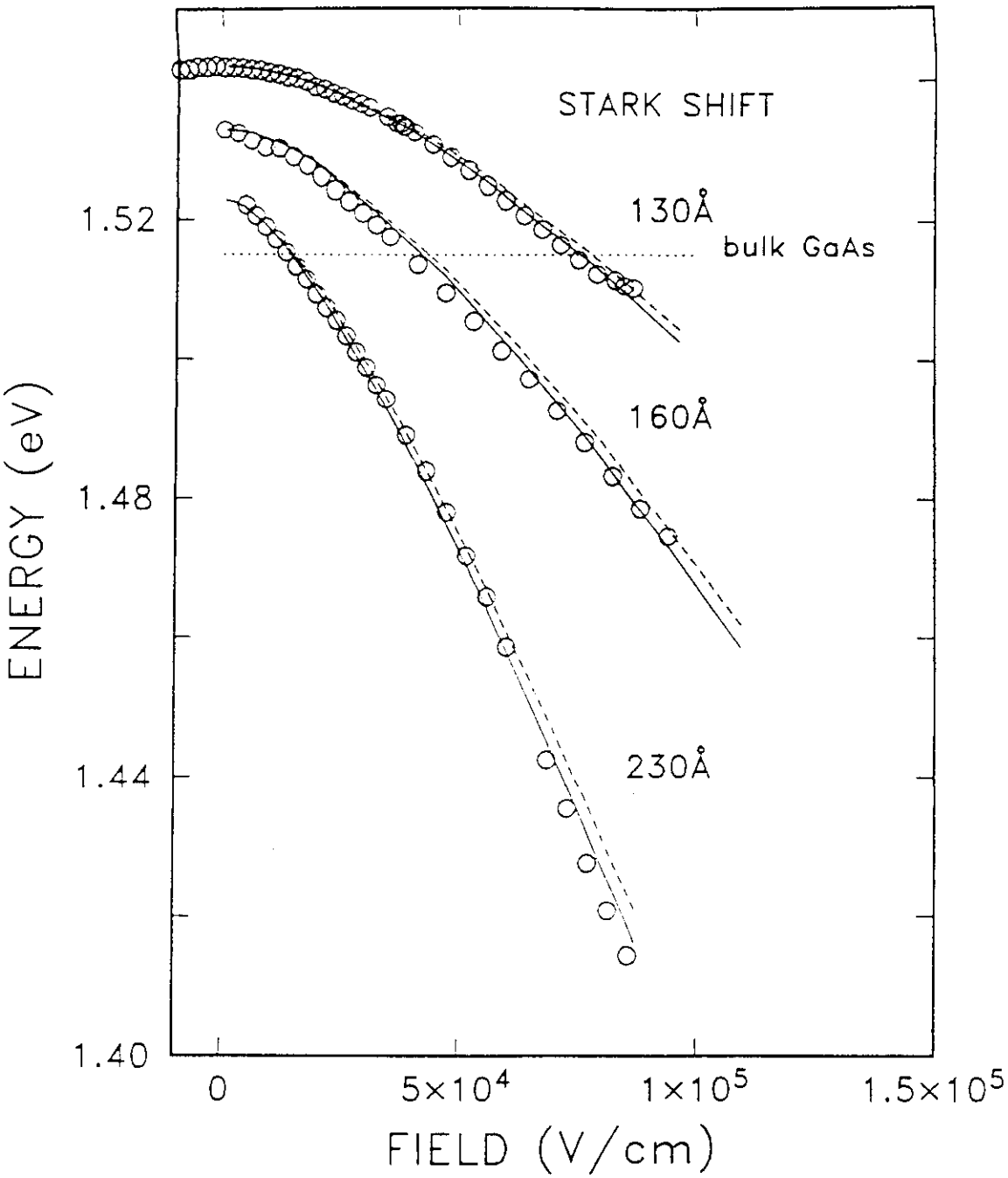
STARK SHIFT
130Å
bulk GaAs
160Å
230Å
1.52
1.48
1.44
1.40
ENERGY (eV)
0
5×10^4
1×10^5
1.5×10^5
FIELD (V/cm)

fig. 149)

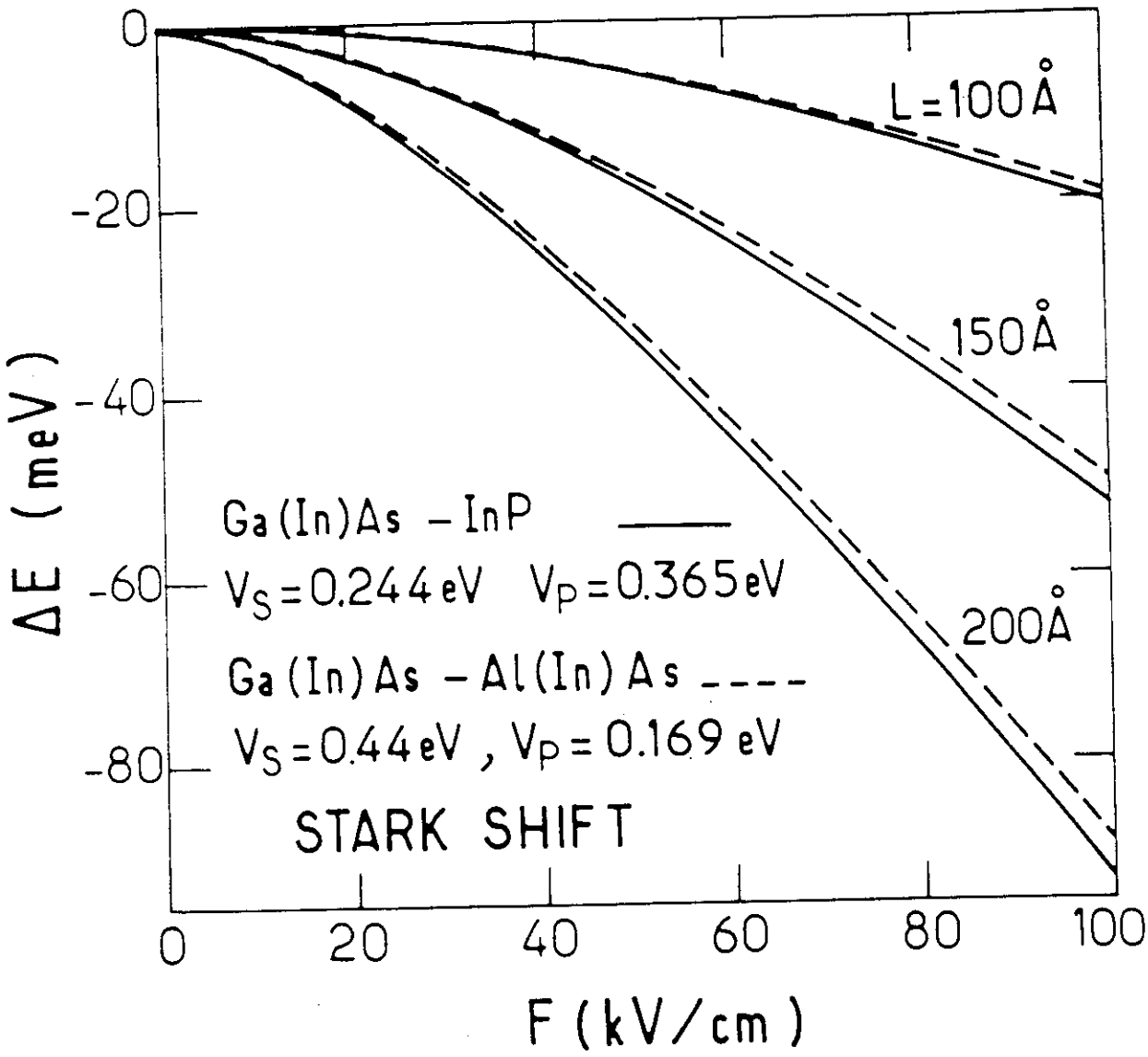
0
-20
-40
-60
-80
ΔE (meV)
L=100Å
150Å
200Å
Ga(In)As – InP
V_S=0.244eV V_P=0.365eV
Ga(In)As – Al(In)As
V_S=0.44eV , V_P=0.169 eV
STARK SHIFT
0
20
40
60
80
100
F (kV/cm)

fig.(50)

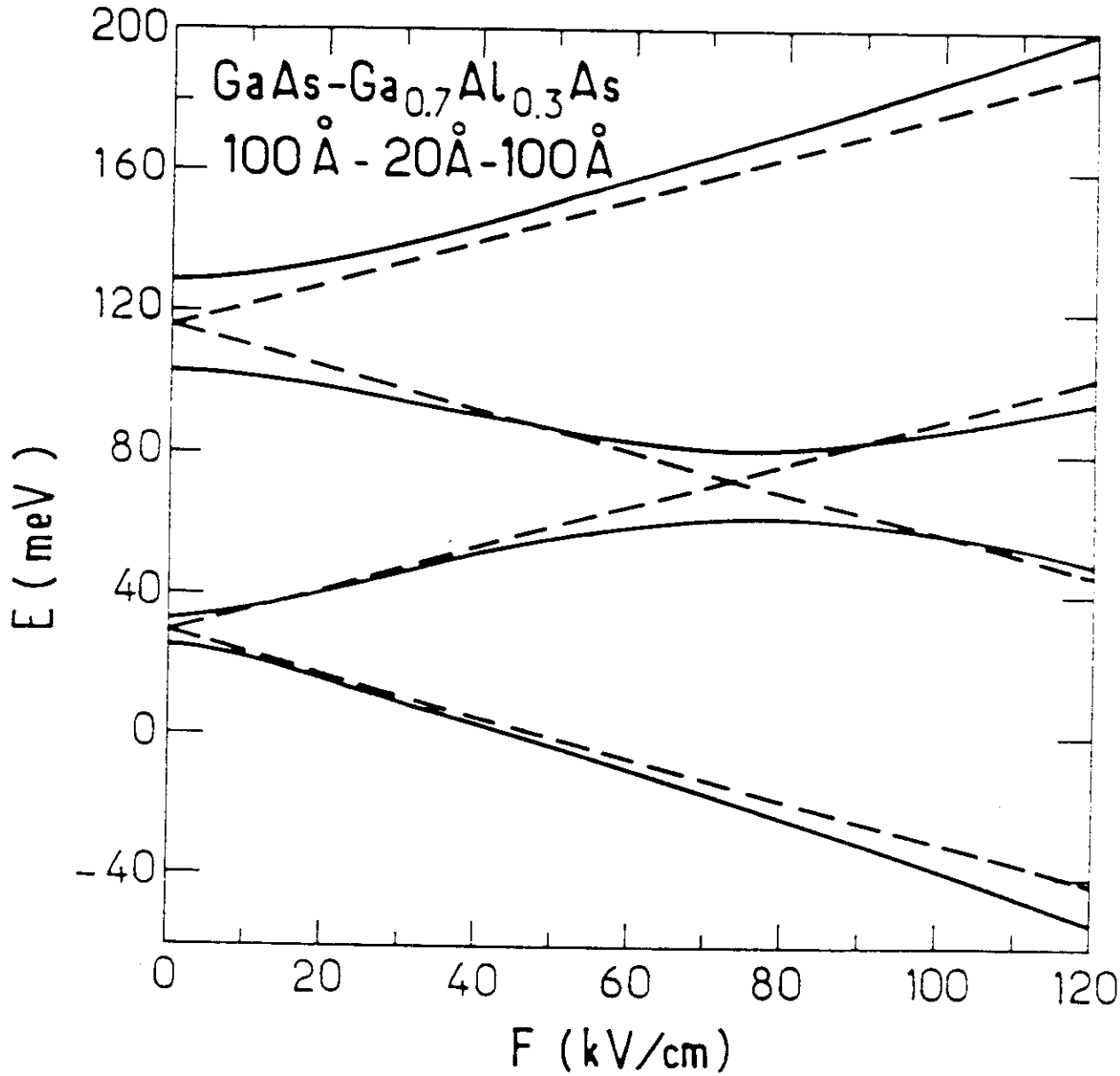
GaAs-Ga0.7Al0.3As
100 Å - 20Å-100 Å
200
160
120
80
40
0
-40
E (meV)
0
20
40
60
80
100
120
F (kV/cm)

fig. (51)

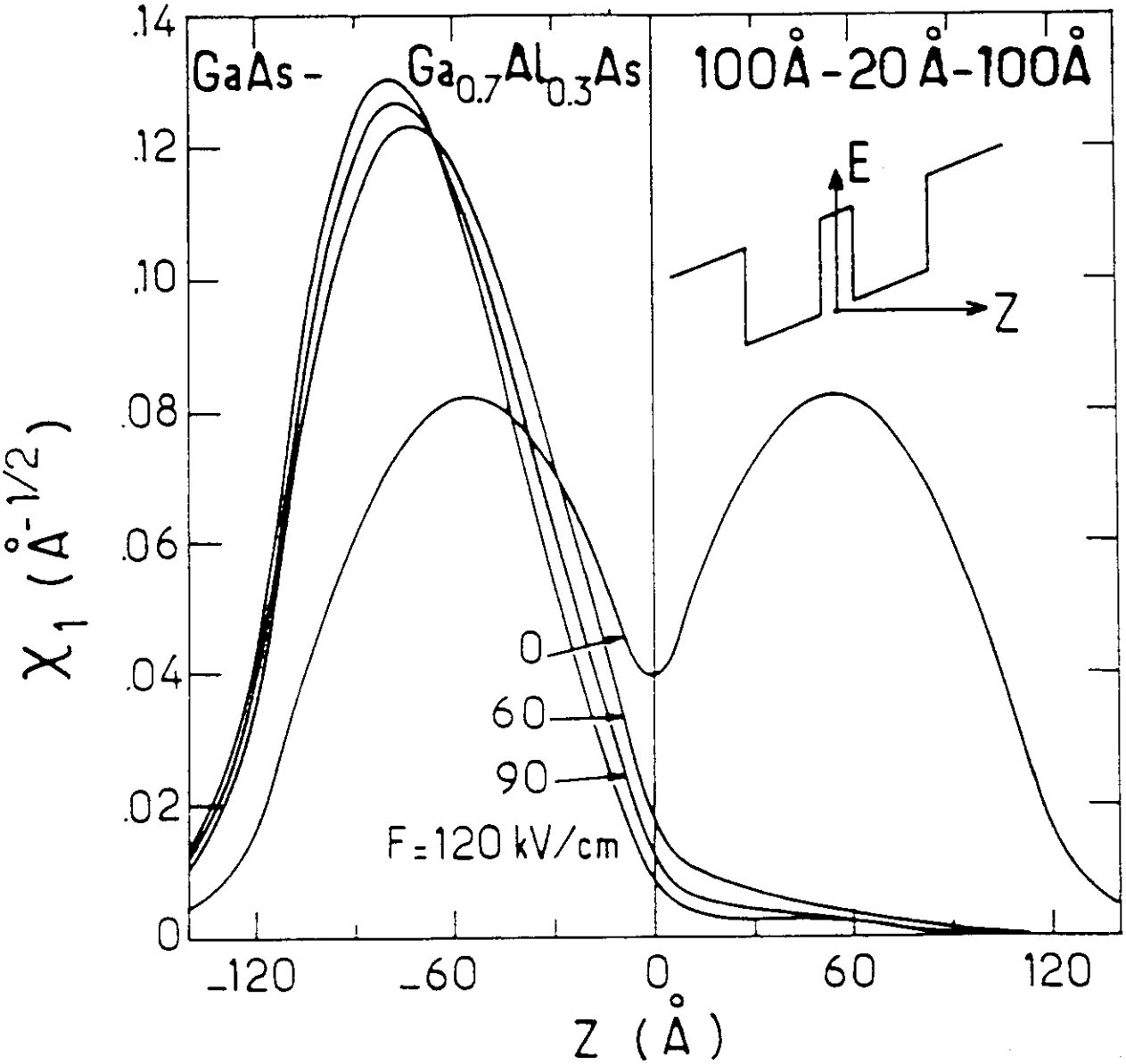
GaAs - Ga0.7Al0.3As
100Å - 20 Å - 100Å
E
Z
0
60
90
F = 120 kV/cm
χ1 (Å-1/2)
Z (Å)
.14
.12
.10
.08
.06
.04
.02
0
-120
-60
0
60
120

fig. (52 a)

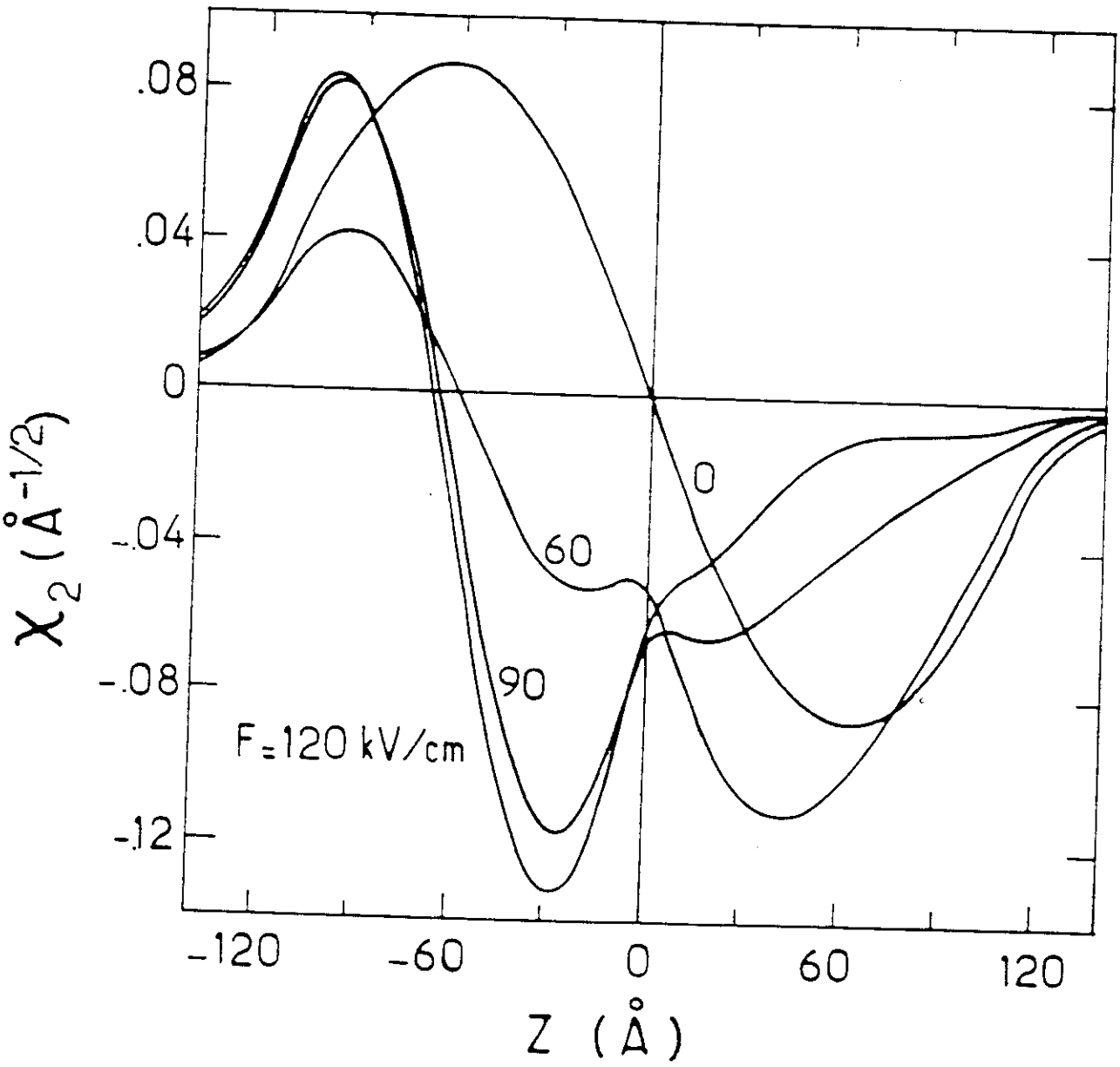

fig. (52b)

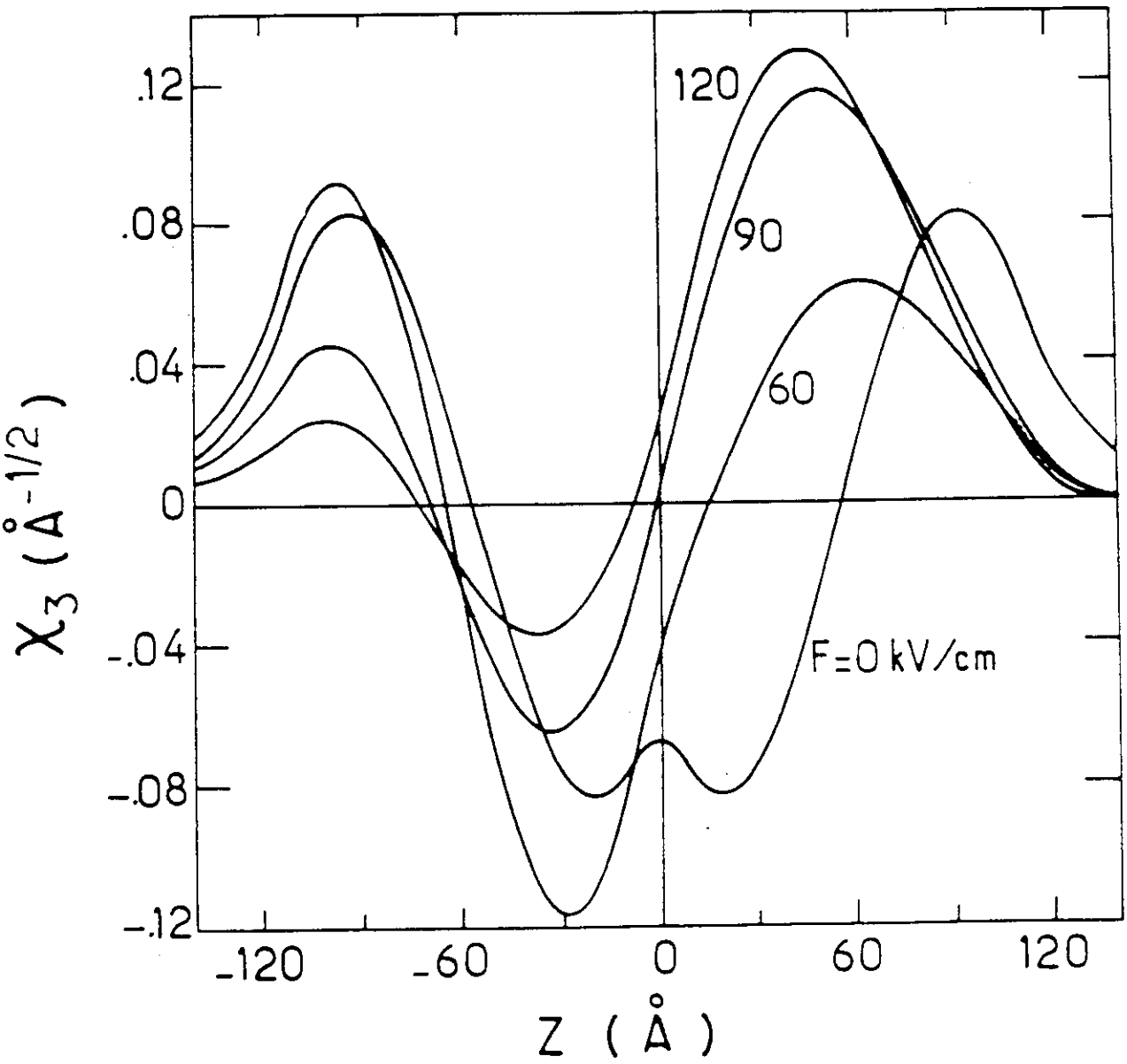

fig. (52c)

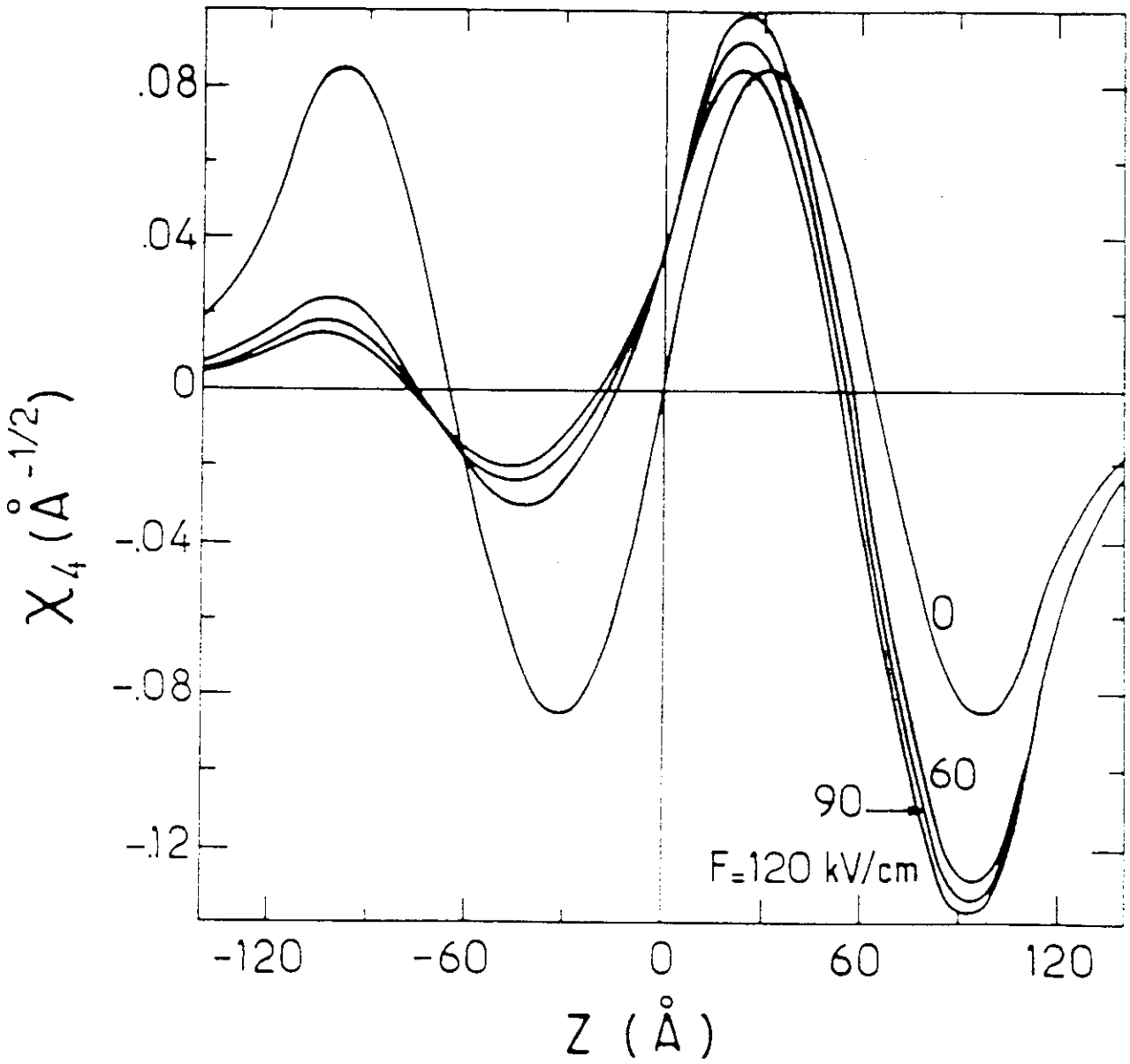

fig. (52 d)

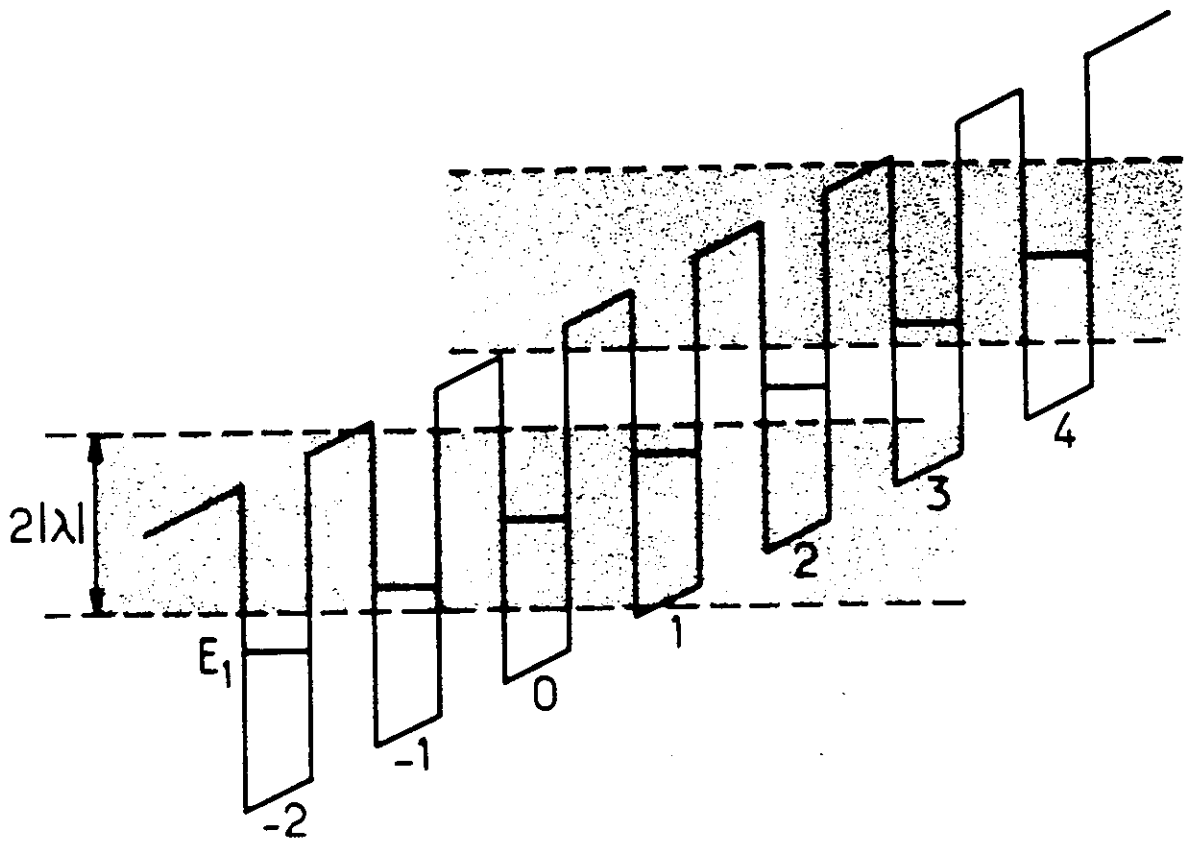

fig. (53)

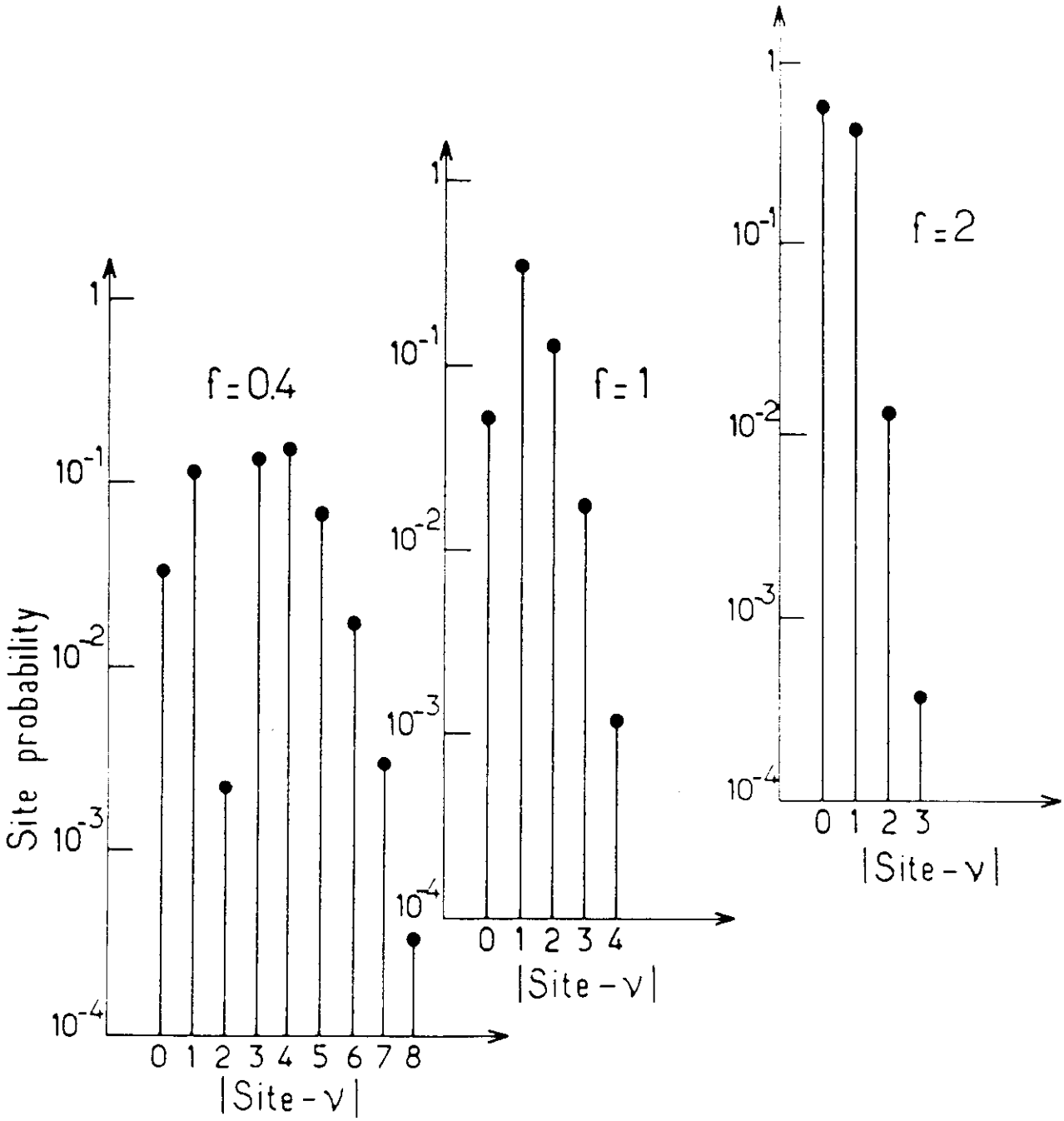
Site probability
1
10^{-1}
10^{-2}
10^{-3}
10^{-4}
f = 0.4
0 1 2 3 4 5 6 7 8
|Site - ν|
f = 1
0 1 2 3 4
|Site - ν|
f = 2
0 1 2 3
|Site - ν|

fig. (54)

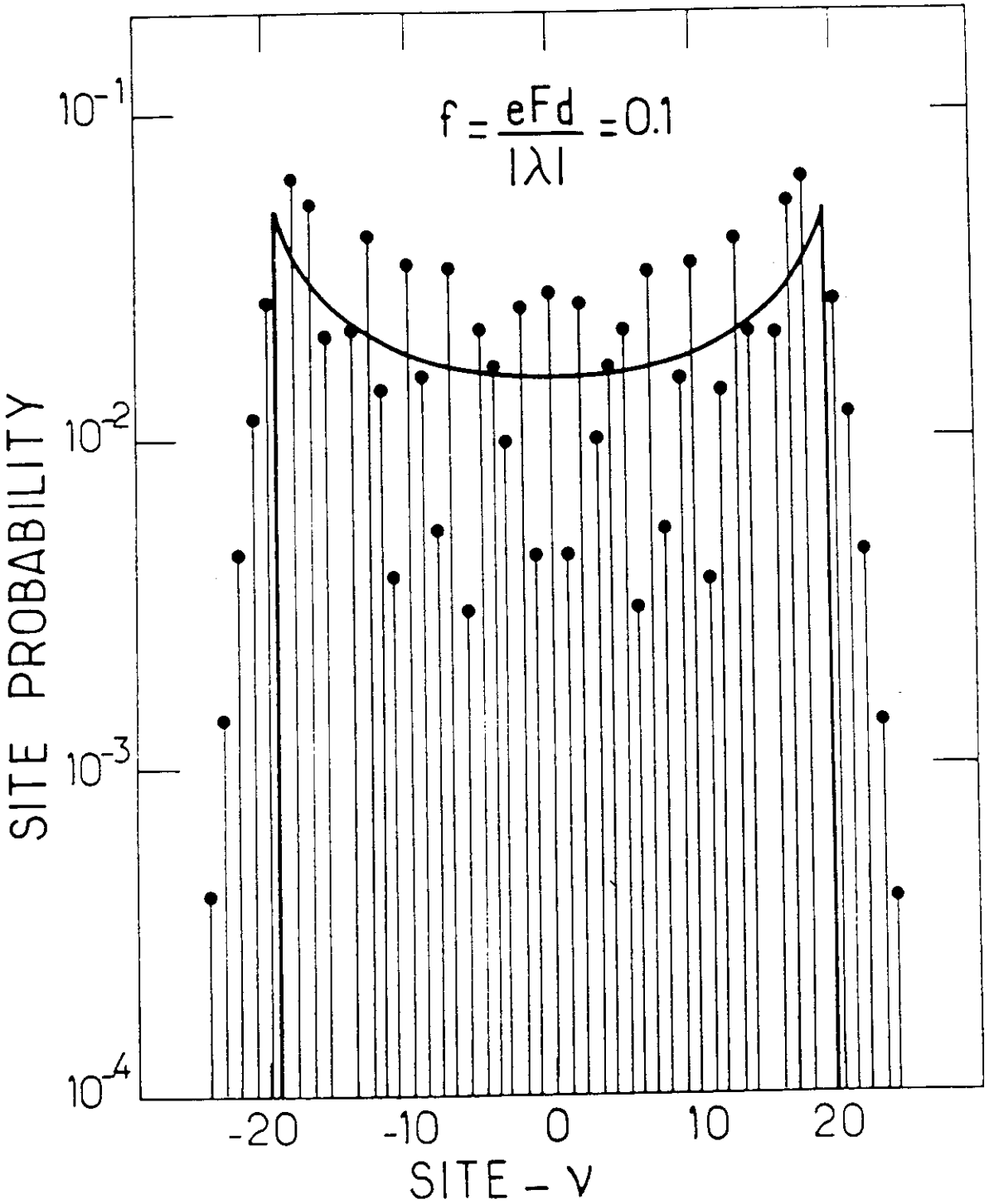
$f = \frac{eFd}{|\lambda|} = 0.1$
10^{-1}
10^{-2}
10^{-3}
10^{-4}
SITE PROBABILITY
-20
-10
0
10
20
SITE – ν

fig. (55)

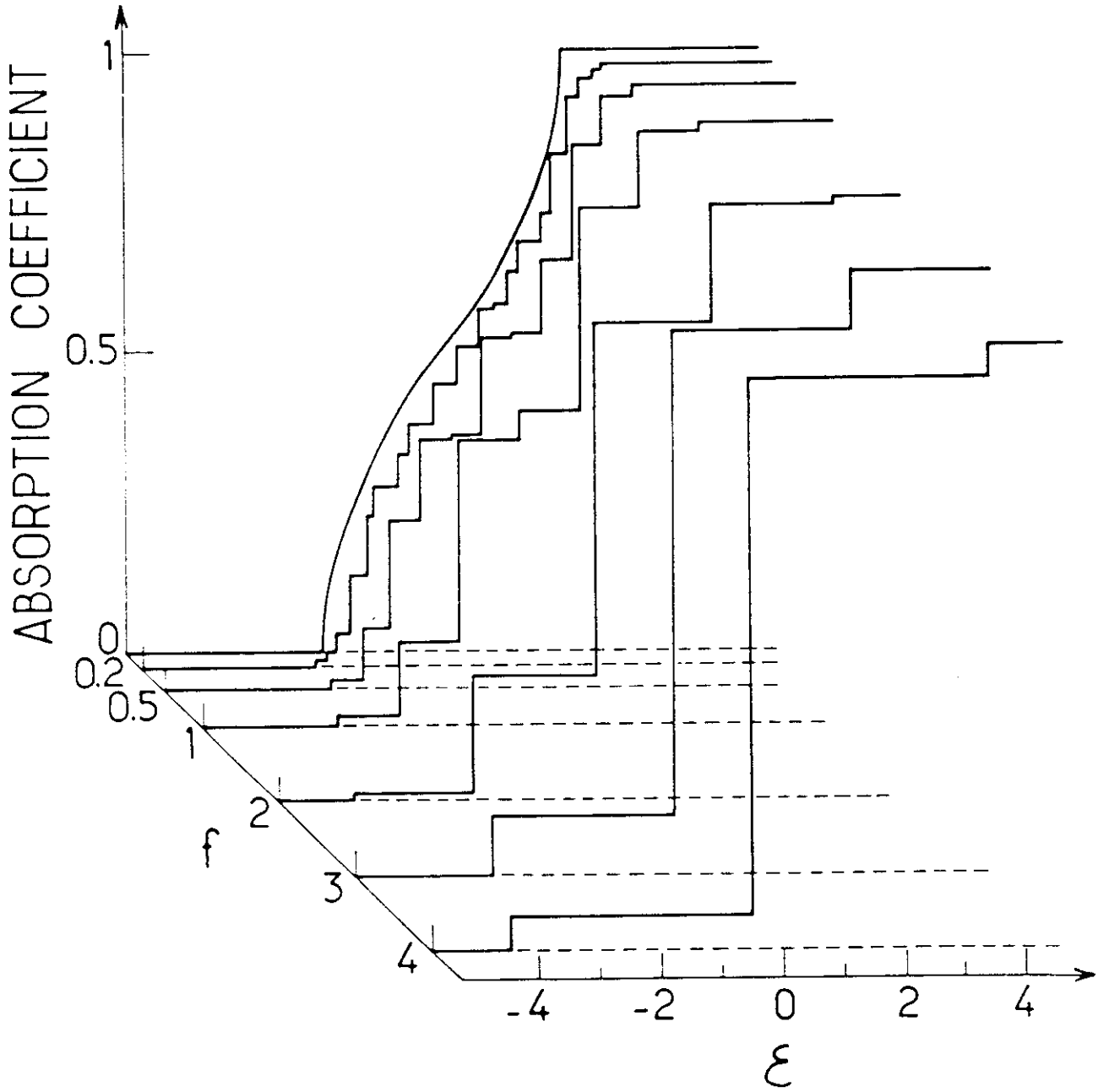

fig. (56)

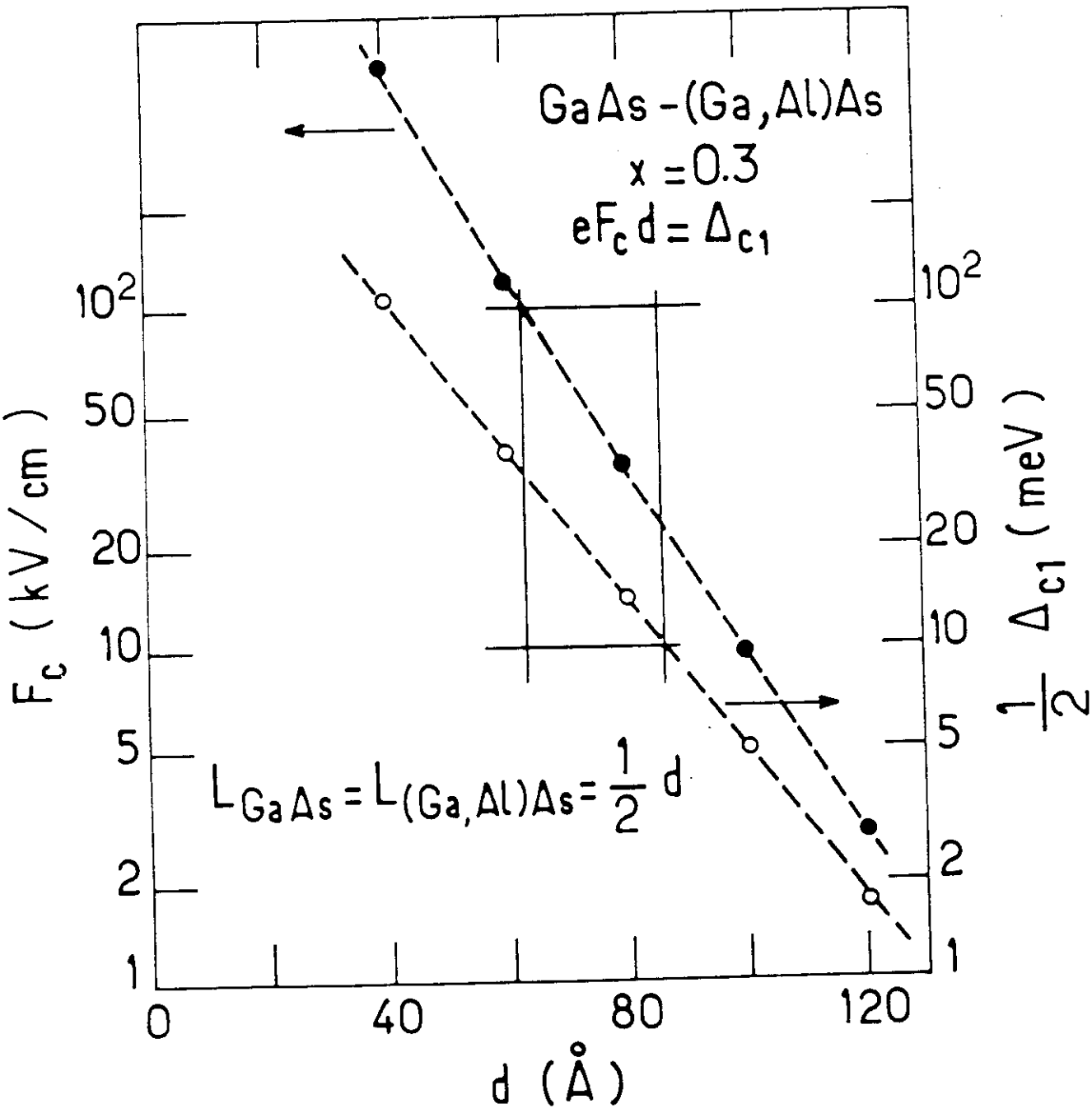
GaAs-(Ga,Al)As
x = 0.3
eF_c d = Δ_c1
L_GaAs = L_(Ga,Al)As = 1/2 d
F_c (kV/cm)
1/2 Δ_c1 (meV)
d (Å)
0
40
80
120
1
2
5
10
20
50
10²

fig.(57)

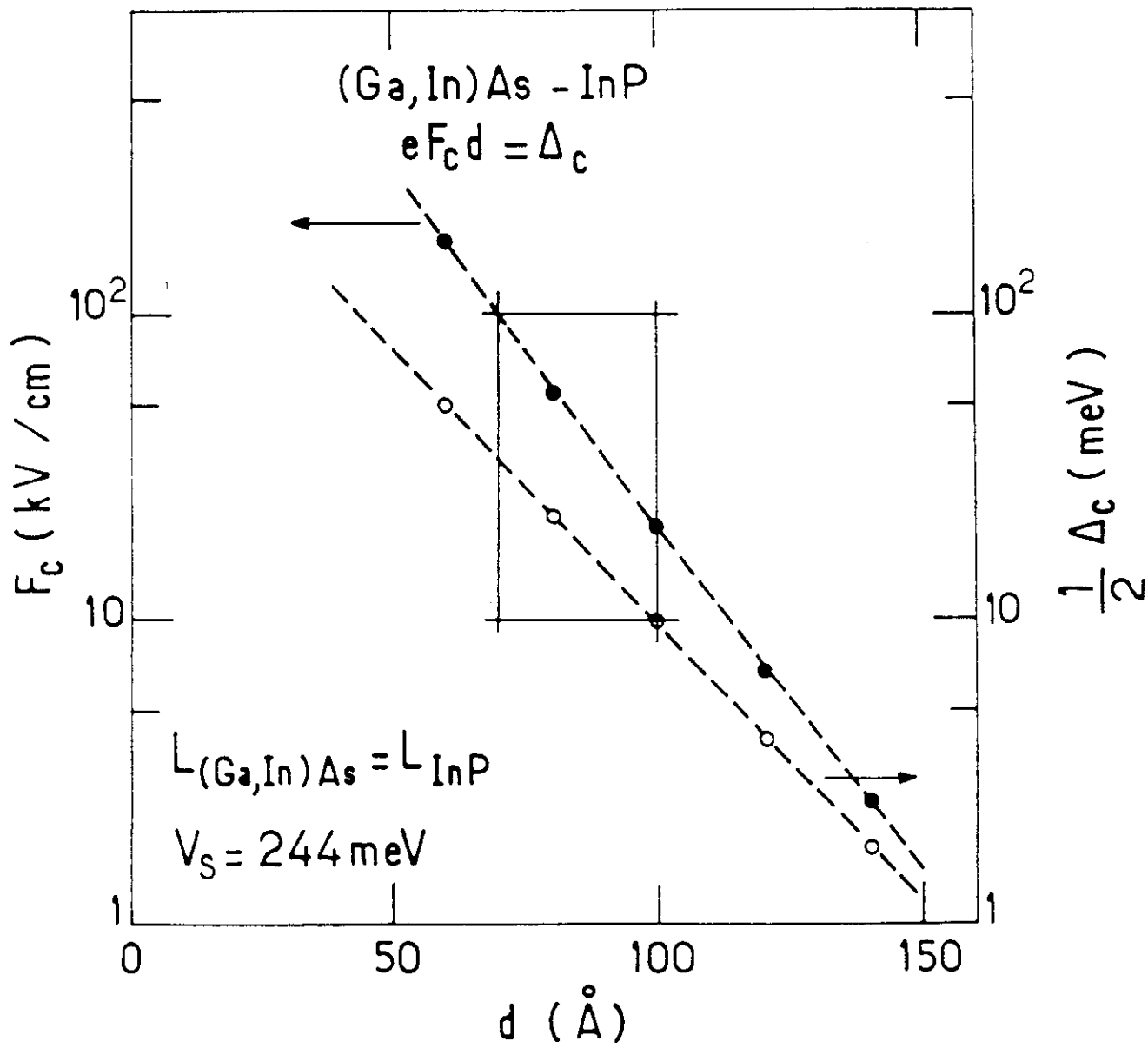
(Ga,In)As - InP
eF_c d = Δ_c
L_(Ga,In)As = L_InP
V_S = 244 meV
F_c (kV / cm)
1/2 Δ_c (meV)
10^2
10
1
0
50
100
150
d (Å)

fig. (58)

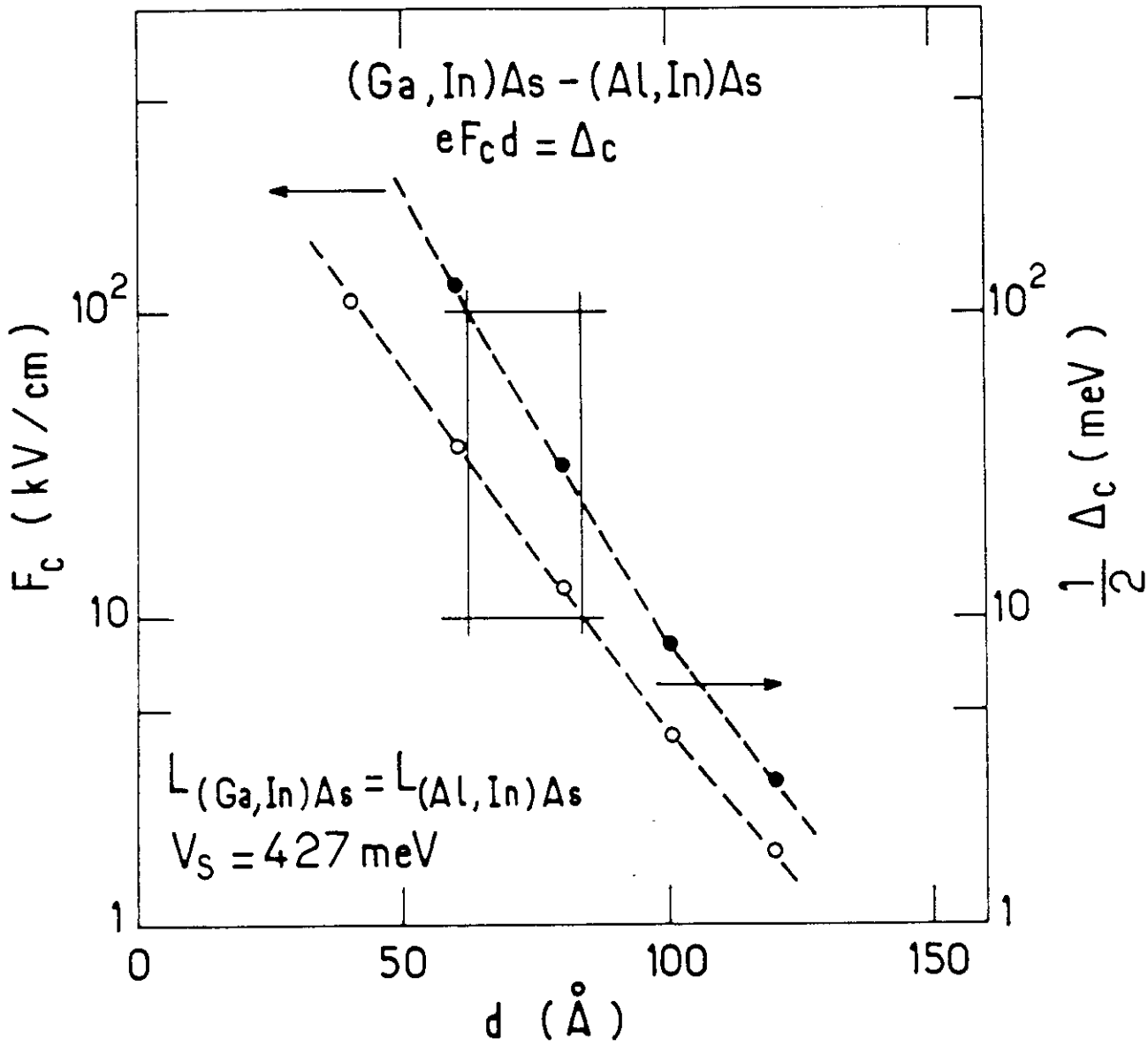
(Ga, In)As - (Al, In)As
eFcd = Δc
L(Ga,In)As = L(Al, In)As
VS = 427 meV
Fc (kV / cm)
½ Δc (meV)
10²
10
1
0
50
100
150
d (Å)

fig. (59)

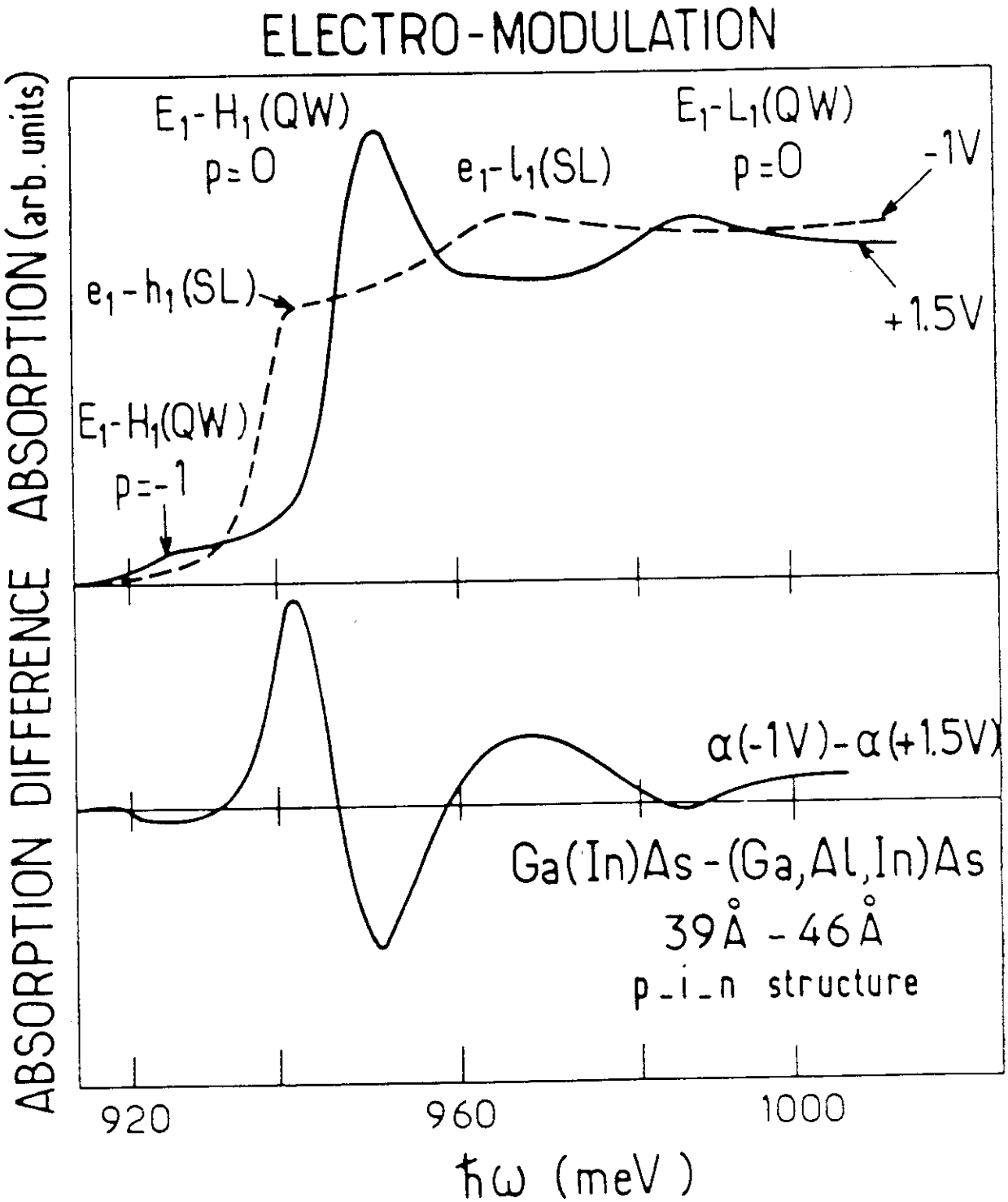
ELECTRO-MODULATION
ABSORPTION DIFFERENCE ABSORPTION (arb. units)
E1-H1(QW)
p=0
e1-l1(SL)
E1-L1(QW)
p=0
-1V
+1.5V
e1-h1(SL)
E1-H1(QW)
p=-1
α(-1V)-α(+1.5V)
Ga(In)As-(Ga,Al,In)As
39Å - 46Å
p_i_n structure
920
960
1000
ħω (meV)

fig. (6c)

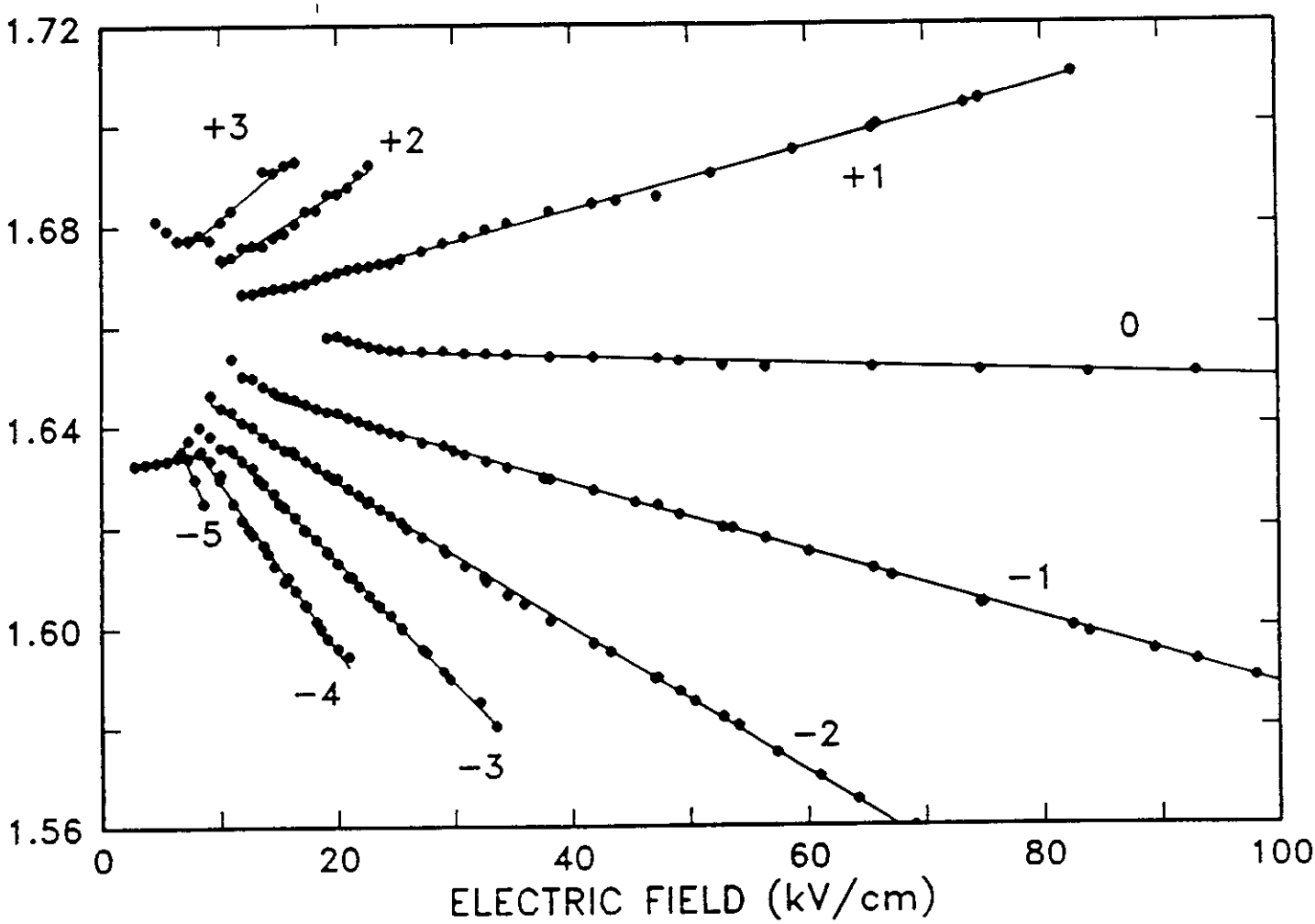
1.72
1.68
1.64
1.60
1.56
0
20
40
60
80
100
ELECTRIC FIELD (kV/cm)
+3
+2
+1
0
−1
−2
−3
−4
−5

fig.(61)

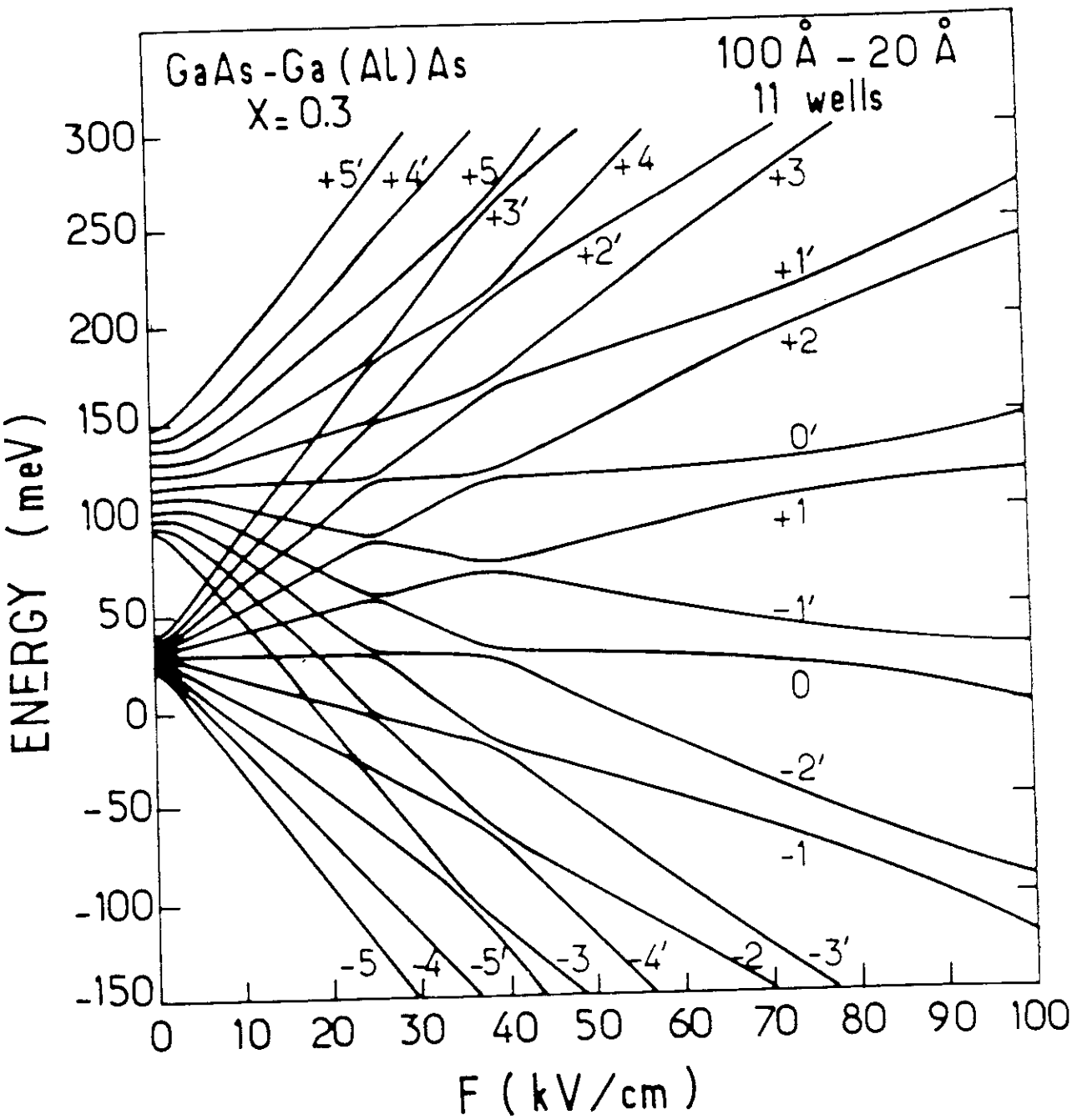
GaAs-Ga(Al)As
X=0.3
100 Å - 20 Å
11 wells
ENERGY (meV)
F (kV/cm)
300
250
200
150
100
50
0
-50
-100
-150
0
10
20
30
40
50
60
70
80
90
100
+5'
+4'
+5
+3'
+4
+2'
+3
+1'
+2
0'
+1
-1'
0
-2'
-1
-5
-4
-5'
-3
-4'
-2
-3'

fig.(62)

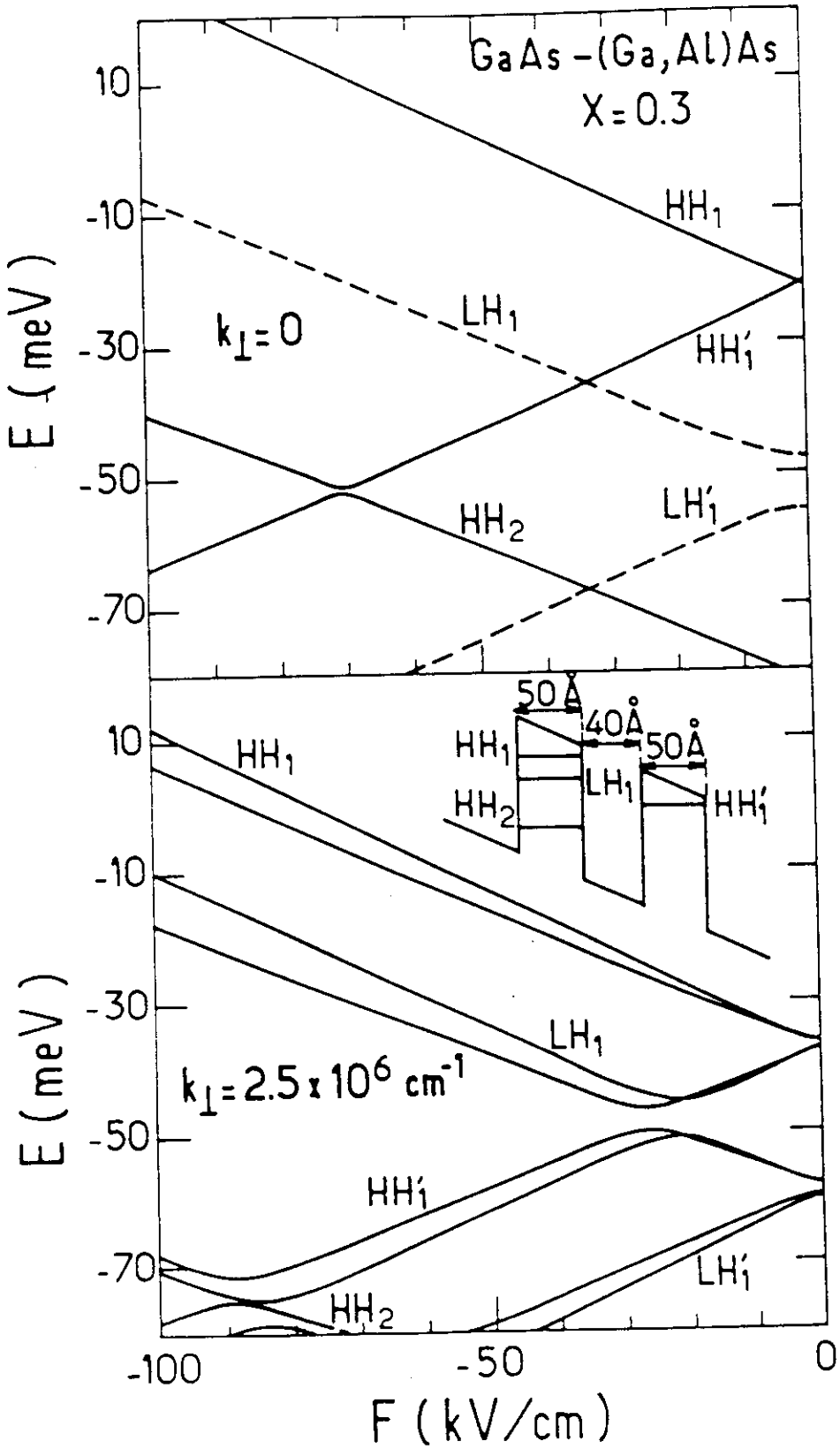
GaAs-(Ga,Al)As
X=0.3
HH1
LH1
HH'1
HH2
LH'1
k⊥=0
E (meV)
10
-10
-30
-50
-70
50Å
40Å
50Å
HH1
LH1
HH'1
HH2
k⊥=2.5x10^6 cm^-1
-100
-50
0
F (kV/cm)

fig.(63)

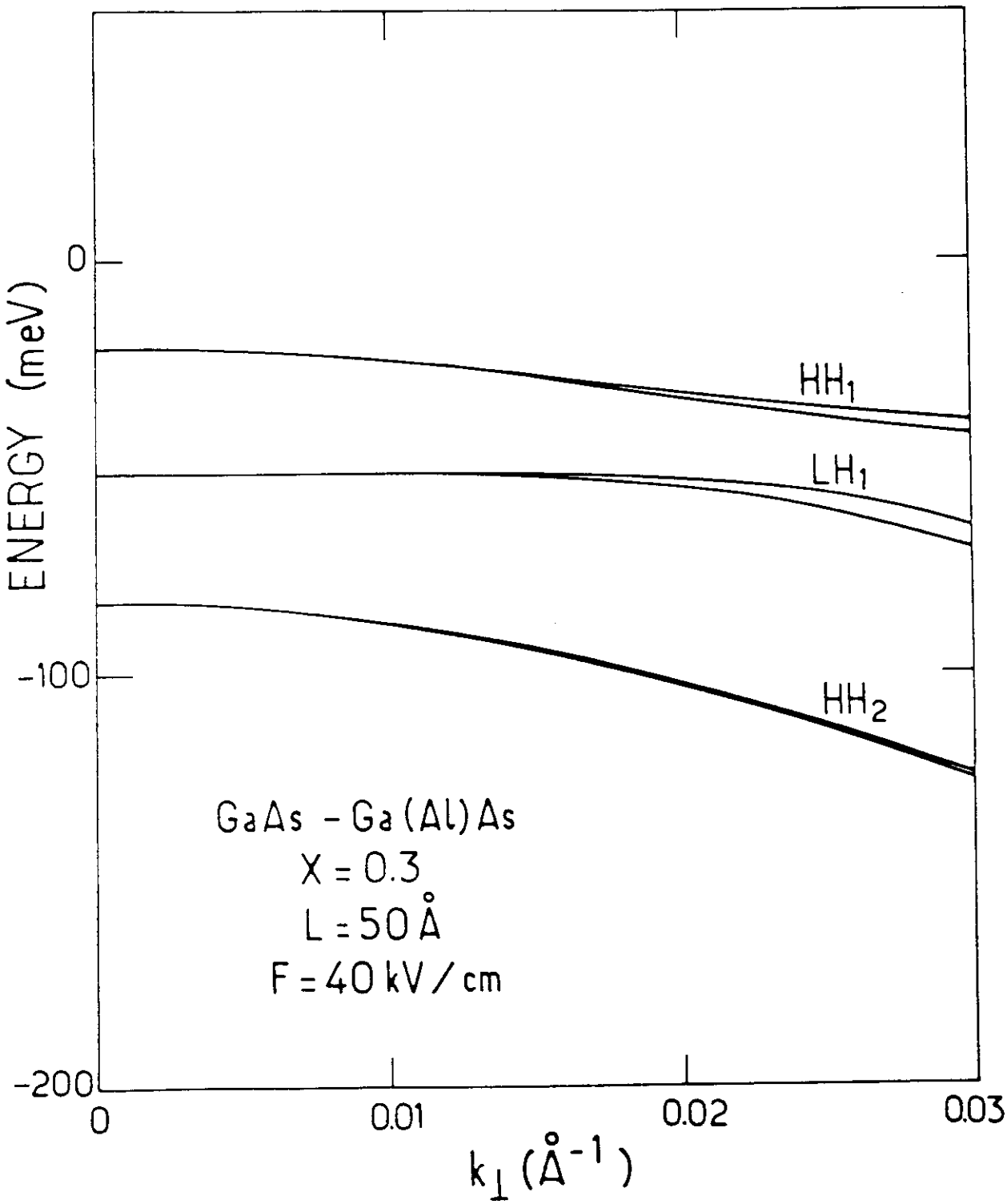
ENERGY (meV)
0
-100
-200
HH1
LH1
HH2
GaAs - Ga(Al)As
X = 0.3
L = 50 Å
F = 40 kV / cm
0
0.01
0.02
0.03
k⊥ (Å⁻¹)

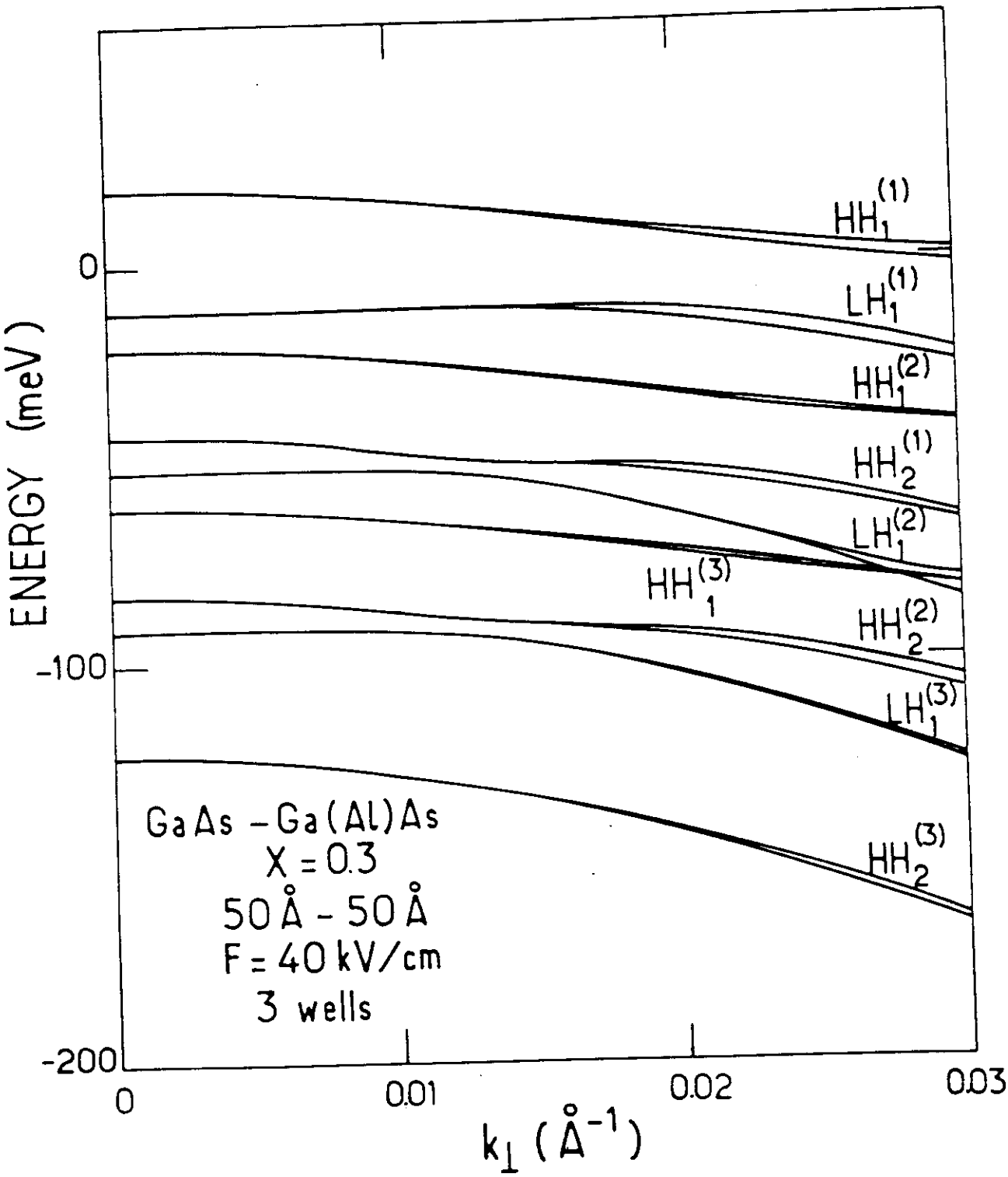
ENERGY (meV)
0
-100
-200
0
0.01
0.02
0.03
$k_\perp$ (Å^{-1})
$HH_1^{(1)}$
$LH_1^{(1)}$
$HH_1^{(2)}$
$HH_2^{(1)}$
$LH_1^{(2)}$
$HH_1^{(3)}$
$HH_2^{(2)}$
$LH_1^{(3)}$
$HH_2^{(3)}$
GaAs – Ga(Al)As
X = 0.3
50 Å - 50 Å
F = 40 kV/cm
3 wells

fig.(65)

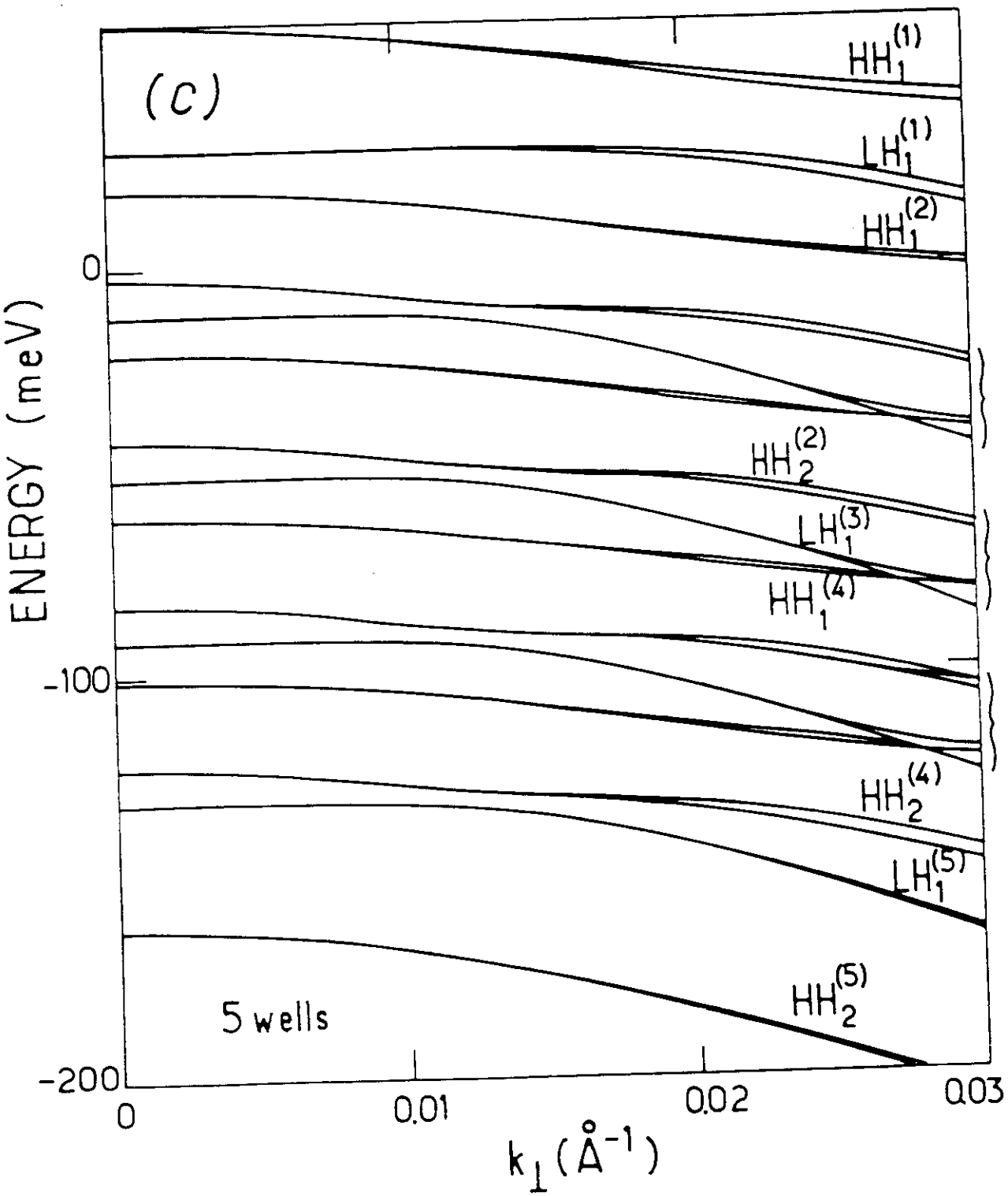
(c)
$HH_1^{(1)}$
$LH_1^{(1)}$
$HH_1^{(2)}$
$HH_2^{(2)}$
$LH_1^{(3)}$
$HH_1^{(4)}$
$HH_2^{(4)}$
$LH_1^{(5)}$
$HH_2^{(5)}$
5 wells
ENERGY (meV)
0
-100
-200
0
0.01
0.02
0.03
$k_\perp (Å^{-1})$

fig. (66)

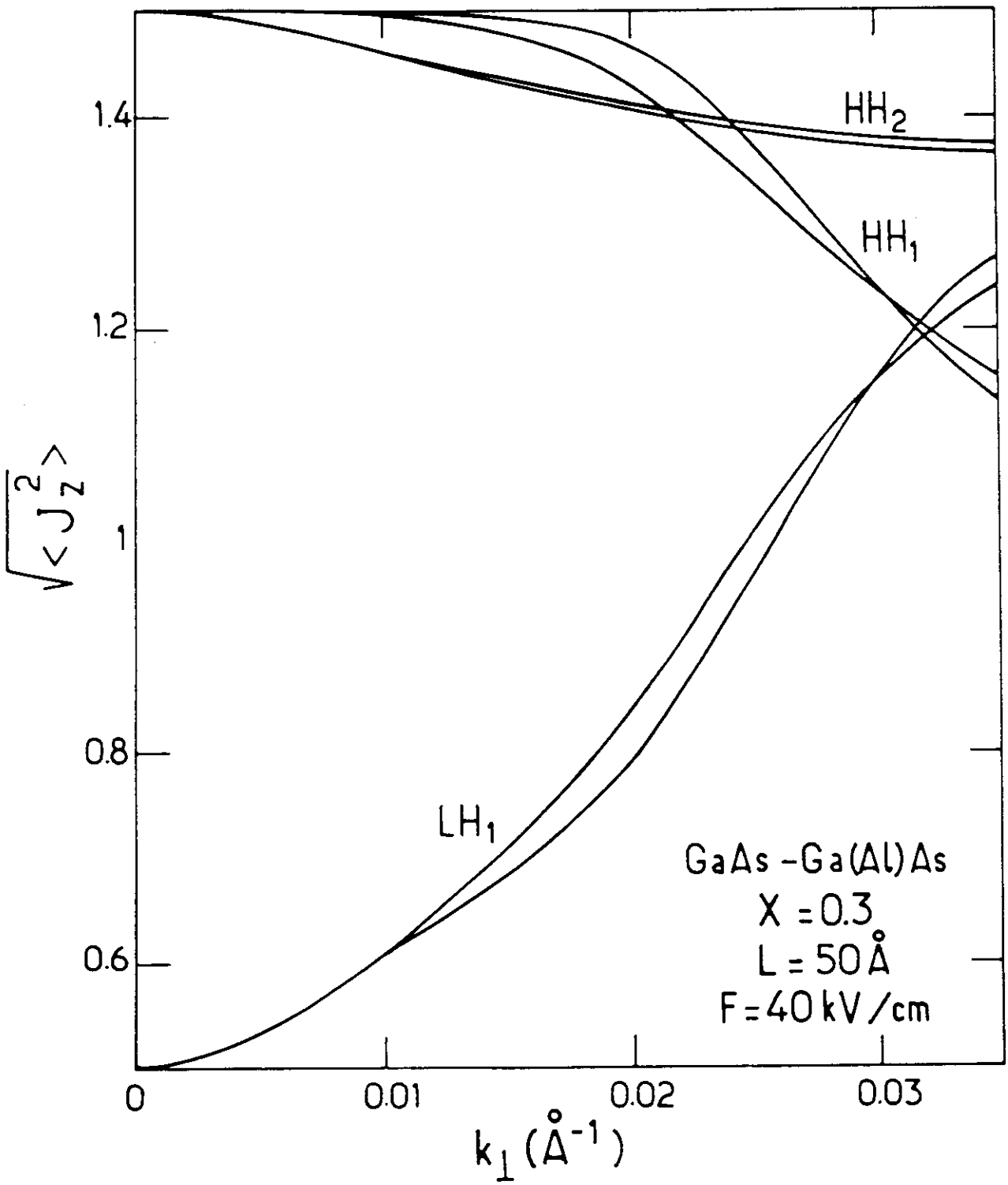
1.4
1.2
1
0.8
0.6
$\sqrt{\langle J_z^2 \rangle}$
HH2
HH1
LH1
GaAs -Ga(Al)As
X = 0.3
L = 50 Å
F = 40 kV/cm
0
0.01
0.02
0.03
$k_\perp$ (Å^{-1})

fig. (67a)

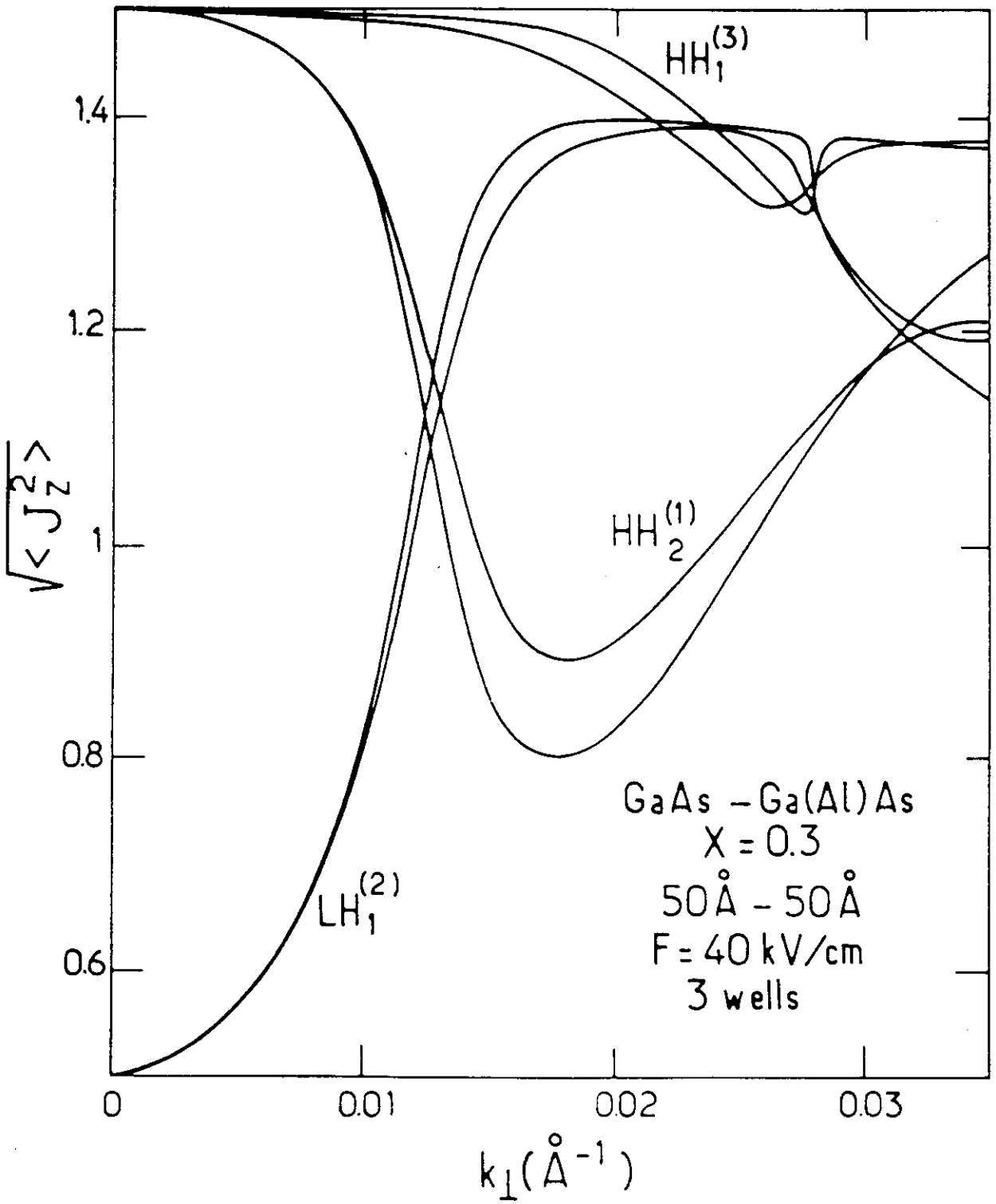
$HH_1^{(3)}$
$HH_2^{(1)}$
$LH_1^{(2)}$
GaAs – Ga(Al)As
X = 0.3
50 Å – 50 Å
F = 40 kV/cm
3 wells
$\sqrt{\langle J_z^2 \rangle}$
1.4
1.2
1
0.8
0.6
0
0.01
0.02
0.03
$k_\perp (Å^{-1})$

fig. (67b)